SSRG International Journal of Civil Engineering
ISSN: 2348-8352/ https://doi.org/10.14445/23488352/IJCE-V13I7P106

Volume 13 Issue 7, 81-116, July 2026

Original Article

Innovation in Construction: Electro-Osmosis for the Durability of Masonry Walls in Coastal Areas

Samuel Bernardo Meza Figueroa[1], Amanda Meza Figueroa[1], Martha Leon Robladillo[1],
Marko Antonio Lengua Fernandez[1*]

[1]*School of Civil Engineering, Universidad Continental, Huancayo, Peru.*

[*]*Corresponding Author : mlengua@continental.edu.pe*

Received: 09 February 2026 Revised: 24 April 2026 Accepted: 16 June 2026 Published: 29 July 2026

Abstract *- Rising damp is one of the main causes of deterioration in masonry walls, due to the capillary migration of water and soluble salts, which causes efflorescence, loss of strength, and, in extreme cases, structural failure. This research evaluated the effectiveness of electro-osmosis as a technique for dehumidification and salt reduction in walls built with pandereta brick, King Kong brick, solid brick, and concrete block. Sixty 1.00 × 1.00 m walls were constructed, previously saturated with 0.5 M NaCl, applying voltages calculated using the Helmholtz Smoluchowski equation and evaluated at 7, 14, 30, 60, and 90 days. Monitoring included moisture measurements and determination of soluble salts in accordance with NTP 339.152:2015, as well as energy consumption and operating costs. The results showed that electro-osmosis reduced the initial moisture content (6.8 to 13.8%) below the hygroscopic value of 2.5% and soluble salts from 1750 to 2300 mg/kg to 470 to 590 mg/kg, classifying it as 'very low saline propensity'. The 14-day prototype interval proved to be technically and economically optimal, simultaneously achieving the reference humidity and minimum salt content with reduced material costs. Over longer periods, the improvements were minimal compared to the increase in time and energy. It is concluded that electro-osmosis is an effective, sustainable, and non-invasive method for controlling rising damp in masonry walls, helping to preserve their durability and prevent deterioration associated with salinity.*

Keywords *- Brick, Electro-Osmosis, Humidity, Soluble Salts, Voltage.*

1. Introduction

Globally, rising damp is one of the main causes of deterioration in building walls, as water rises through capillary action, carrying soluble salts which, when crystallised, cause efflorescence, plaster detachment, and loss of strength in materials, effects that are intensified in environments with high relative humidity [1, 2]. In Peru, the problem is particularly critical on the coast, where chloride-laden sea breezes and constant fog increase humidity and accelerate degradation [3]. Although rainfall is low, the average annual relative humidity reaches 85%, compared to 60% in the mountains and 90% in the jungle [4]. These conditions cause efflorescence, cracks, and progressive loss of structural strength to appear on walls, particularly those built with clay bricks and concrete [5-7].

In Lima, this damage has led to critical situations, such as the collapse of homes in Barrios Altos in July 2024, where moisture accumulation caused the collapse of block 1 of Jirón La Mar, affecting nearly 20 families [8]. Similarly, districts such as Chorrillos, Villa María del Triunfo, and San Juan de Lurigancho have reached relative humidity values between 98% and 100%, intensifying the feeling of cold, facilitating the growth of molds and respiratory diseases, and increasing metal corrosion [9] and concrete deterioration. Punta Hermosa was selected as the priority coastal district for the study because visible damage in walls and finishes affects over 60% of homes at the coast, and nearly 40% of the urban front directly adjacent to the coast is classified as 'very high' vulnerability to humidity and salinity [10]. According to national censuses, 55.8% of homes in Peru used brick or cement blocks as the predominant material in their walls [11].

Figure 1 shows this distribution: the pandereta brick achieved the highest share with 39%, followed by the 18-hole King Kong with 29%, while solid bricks accounted for just 3% [12-14]. In addition, recent studies have projected growth in the use of concrete blocks (up to 29% in Lima) due to their seismic resistance, lower mortar consumption, and cost reduction [15].

Therefore, this research analysed pandereta, King Kong, solid and concrete bricks, with the aim of evaluating their behaviour in relation to humidity and their response to treatment by electro-osmosis, guaranteeing results that are applicable in real urban scenarios in the country.

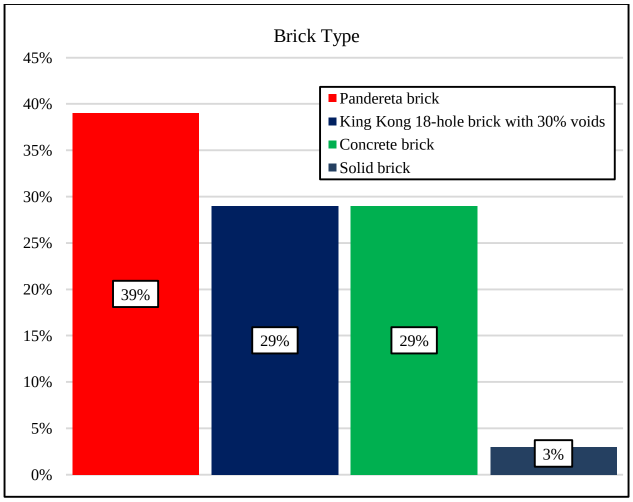

Fig. 1 Representative bricks in walls in Peru

In this context, there are various methods of controlling humidity in buildings, such as the application of waterproof coatings, the incorporation of perimeter drainage systems, and even the installation of physical anti-capillary barriers, which have limitations due to their invasive nature, high maintenance costs, or poor durability in the face of high coastal salinity [16, 17]. However, electro-osmosis is emerging as an innovative alternative, as it acts directly on the water contained in the pores and capillaries of building materials [18]. In order to aid moisture crystallisation damage and reduce moisture build-up caused by the movement of water to the anode and then cathode, direct electric currents are used as a part of this physical chemical process [19]. While still in an early stage in Peru, its worldwide use in the last three decades has proved to be 80% effective within the field of dehumidification of historic buildings, museums, and homes, with the preservation of coatings, conservation of maintenance, and conservation of inestimable heritage value [20, 21]. However, the literature has mainly focused on electro-osmosis in heritage or uniaxial material contexts; the performance of which has not been compared across masonry units under equivalent conditions. In the Peruvian context, this limitation is particularly relevant since in the coastal environment, exposed to high humidity and salinity, heterogeneous types of bricks that are still poorly documented with regard to their differential response to electro-osmotic treatment coexist among mudbricks. Besides being technically effective, this technology is also environmentally friendly and economical because it does not require extensive chemical use and minimizes the remaining of structures' pores [22]. Through this, the novelty of this research lies in systematically comparing the effectiveness of four representative masonry materials (pandereta, King Kong, solid brick, and concrete block) by placing them under identical conditions for the evaluation of both moisture reduction and soluble salt removal. Under this premise, this research evaluated the efficiency of electro-osmosis in reference prototypes made of clay for the main types of bricks used in Peru (pandereta, King Kong, solid, and concrete block) [12], under controlled conditions of salt saturation; thus obtaining a basis to validate experimentally and its contribution as a technique viable scalable sustainable solution for conservation and durability buildings on coastal areas. To bridge this gap, the present work provides comparative evidence to support better material selection for electro-osmotic applications in a coastal urban environment. Thus, its adoption could become a reference model for technological solutions applicable in regions with similar climatic and construction conditions, opening up opportunities for housing conservation projects, sustainable urban development, and mitigation of the impacts associated with humidity and salinity on infrastructure. In order to contextualise this research, a review of previous studies on the application of electro-osmosis in walls affected by rising damp was carried out.

2. Literature Review

2.1. Electro-Osmosis in Historic and Heritage Buildings

In Turkey, the Department of Mechanical Engineering at Istanbul Technical University, in collaboration with the Faculty of Engineering at Istanbul Kültür University, carried out an applied study at the Gül Mosque in Istanbul, a historic building affected by rising damp. To this end, an electro-osmosis system was implemented by installing a capillary repulsion device and strategically placing electrodes in the walls. The methodology consisted of taking systematic moisture measurements at different heights and depths of the walls, using a Gann hygrometer, over a period of more than five years. The analysis demonstrated an effective treatment that changed the water content of the walls from an initial 14.48% to 2.90% in just 9 months. This signified a transition from 'very damp' to 'dry,' and the water loss reduced the thermal conductivity of the walls by 58% [21]. Another study from the Environment Department of Istanbul Technical University used electro-osmotic methods on a damp 18th-century European heritage building. The walls of the ground floor had severe damp issues. The result was a sustained progressive decrease in the moisture. In the first 6 months, the damp patches and salt efflorescence diminished, and in 1 year, the moisture content was reduced to safe levels for the material's stability. In addition, the process did not damage the historic structure, nor did it require any invasive measures, confirming that electro-osmosis can be used instead of traditional methods such as chemical injections or physical cuts in the walls [22].

In Aveiro, Portugal, the Department of Civil Engineering at the University of Aveiro, in collaboration with the University of Porto, conducted applied research on the Twin Churches of St. Anthony and St. Francis to assess the feasibility of the active electro-osmosis technique in treating rising damp in stone walls. The methodology included preliminary inspections, installation of a system of titanium electrodes connected to a power unit, and systematic monitoring using hygrometers, thermal imaging cameras, and gravimetric laboratory tests. The results obtained showed a significant decrease in moisture content: over a period of ten weeks, the values went from 12.53% to 9.94% and from 10.85% to 8.72% according to gravimetric tests, confirming an approximate reduction of 2.3% during that period. These findings demonstrated the effectiveness of the technique in historic buildings, highlighting that, although it requires a high investment and long-term results, it offers the advantage of permanent elimination of the pathology as long as the system remains in operation [24].

2.2. Experimental and Material-Based Studies on Electro-Osmosis

The Belgian Building Research Institute (BBRI) examined the application of active electroosmotic techniques to control rising damp in historical buildings. Anodes were placed in the walls of a typical Walloon house with schist walls one metre thick. (Cathodes were placed in the ground.) Monitoring was done with analysis of the drilled and extracted dust, as well as the recorded moisture. At the end of six months of electroosmotic treatment, the moisture content in the upper wall was reduced from 7.5 to about 6 percent. At the base of the wall, moisture content increased from 8 to about 10 percent due to the seasonal changes monitored [19].

In Denmark, an experimental study conducted by the Technical University of Denmark (DTU Sustain) focused on electro-osmosis on both modern and historic bricks. Four types of bricks contaminated with NaCl were analysed, and the parameters porosity, zeta potential, and transport coefficients were obtained. Electro-osmosis was found to be very effective on Dalum bricks with an electro-osmotic permeability coating (L_{12}) of 3.68×10^{-10} m²/V·s and a chloride diffusion coating ($D_{e}ff\ Cl^{-}$) of 1.27×10^{-11} m²/s, decreasing chloride by 58% and nitrate by 83%. Other bricks, such as Horsens, achieved reductions of 9% with a much lower L_{12} (8.80×10^{-11} m²/V·s). These results confirmed electro-osmosis as a potential candidate for moisture and salt reduction for the conservation of historic buildings [23].

Research at the Aldo Pontremoli Department of Physics, State University of Milan, Italy, studied the application of electro-osmosis on building materials to mitigate damage from rising damp. The study focused on different specimens of brick, lime mortar, cement, and lime mortar, and brick dust plaster (cocciopesto), saturated with water and NaCl saline solution, to which direct electric fields of up to 30 V/m were applied. The methodology included measurements of moisture content using gravimetry, infrared thermography, and optical reflectance in the 970 nm band, comparing drying with and without the application of electric current. The results showed that there were no significant differences in the distribution or kinetics of moisture drying between the samples subjected to an electric field and those that were not, even with voltages ten times higher than those used in commercial systems. Only under extreme conditions of 150 V/m was a localised increase in temperature observed near the electrodes due to the Joule effect, with no evidence of effective electro-osmotic water flow [20].

2.3. Technical Limitations and Influencing Factors

In Bologna, Italy, the Department of Civil and Materials Engineering at the University of Bologna conducted a review of rising damp control focused on electro-osmosis in historic walls; the methodology consisted of analysing 65 publications up to 2017. In the experimental cases reported, water movement was documented in brickwork with currents of 0.16 to 0.47 mA/cm electrode applied for 9 days, although drying was insufficient. Moreover, in a Russian building, a marked decrease in humidity was observed when 200 V was applied for 4 months and then 150 to 160 V for 3 months (intervention only feasible without occupation due to high voltages). The study concluded that effectiveness depended heavily on the microstructure (pore size), the chemistry/pH of the medium, and electrical continuity affected by material rigidity and possible anodic acidification, and therefore recommended case-by-case validation on actual walls and the use of monitoring instrumentation to quantify moisture reductions under specified electrical parameters [18].

In Stockholm, Sweden, the Department of Civil Engineering conducted applied research on the use of electro-osmosis to manage moisture problems in foundations and basements. The methodology included a literature review, process modelling, and field visits to five buildings where electro-osmotic systems had been installed. In these installations, silver- or gold-coated titanium anodes were placed in holes drilled in the walls and cathodes in the ground, connected to an electronic unit that applied a pulsating voltage of approximately 20 V for 30 seconds, reversed for 3 seconds, and followed by 10 seconds of rest, with currents reaching values close to 200 mA. The reported results showed improvements in interior conditions and reduced damage to stored objects, confirming the potential of the technique. However, the study highlighted that electro-osmosis requires the capillaries in the concrete to be saturated (internal relative humidity $\geq$ 80%) to be effective and that, although it can significantly reduce moisture in walls, it needs to be complemented by other drying methods to achieve levels below the critical threshold for mould and rot [25].

In China, the Key Laboratory of Road and Traffic Engineering of the Ministry of Education at Tongji University (Shanghai) conducted research to evaluate the effectiveness of electro-osmosis in subgrade soils, comparing Iron Electrodes, Graphite Electrodes, And A New Electro-Geosynthetic Electrode (EKG) made from drainage pipes wrapped in carbon fibre. The methodology included laboratory tests with gradients of 0.8, 1.0, and 1.2 V/cm, as well as a meso-scale field test powered by solar energy for one month. The results showed that electro-osmosis reduced soil moisture content by between 8.5% and 15.4%, with the EKG being the most efficient at reducing moisture in the top layer by up to 12% in one month, while in the untreated sample, it increased by 3.7% due to rainfall. In addition, this new electrode reduced the contact resistance between the soil and the electrode by 19.7 to 40.8% and performed better against corrosion, while the iron electrodes reached contact resistances up to 4.1 times higher, confirming that the EKG is more suitable for long-term applications in subgrade stabilisation using electro-osmosis [26].

2.4. Alternative Methods for Moisture Control and their Limitations

In a scientific review conducted by researchers from the National Research Council Canada and the University of Ottawa, the main mechanisms of moisture ingress into building envelope materials capillarity, vapour diffusion, and condensation were analysed, as well as the most widely used techniques internationally to mitigate these effects, including the use of drainage systems and waterproof coatings, the installation of vapour barriers and mechanical ventilation, the selection of moisture-resistant materials, and the application of hygrothermal simulations to predict the performance of walls under different environmental conditions. However, despite their contribution, these methods have shortcomings: drainage systems require continuous maintenance, vapour barriers can trap moisture if placed on the wrong side of the wall, and hygrothermal simulations rely on ideal models that do not always represent actual construction conditions [16]. Similarly, another scientific review conducted by researchers at Jilin University in China analysed the applications of capillary barrier coatings in various fields of engineering, including landfills, nuclear waste repositories, tailings dams, slope protection, road sub-bases, and agricultural use. Covers have demonstrated the ability to minimize the penetration of water, control the migration of salts and oxygen, reduce the generation of acid mine drainage, and enhance the stability of slopes. Even though the results are quite positive, the authors of the study highlighted some limitations. These include the reliance on certain climatic conditions (they may perform poorly where there are heavy rainfalls in humid regions), the elaborate process of designing the cover and choosing the materials (which needs considerable variation in the hydraulic conductivities of the layers), the expensive solutions due to the need for more complex, multi-layered systems, and the requirement of considerable long-term monitoring and maintenance to be able to perform stably over time [17].

2.5. Identified Research Gap and Justification of the Study

Despite the extensive international research on electro-osmosis and alternative moisture control methods, most studies have focused on heritage buildings, specific materials, or controlled laboratory conditions, without addressing the comparative performance of multiple masonry units commonly used in contemporary urban housing. Furthermore, although previous studies identified key influencing factors such as porosity, voltage, and material composition, these parameters have not been systematically evaluated under equivalent experimental conditions in the context of Peruvian coastal environments, characterised by high humidity and salinity. This constitutes a major research gap, because there is no experimental evidence in the literature scaling up both electro-osmosis on different masonry materials and reducing moisture and soluble salts of major masonry materials currently used in Peru. This conceptual shortage encouraged the current work to prospectively analyze electro-osmosis in prototype walls manufactured with some normal masonry materials for Peru: pandereta brick, 18-hole King Kong bricks, solid brick, and concrete blocks. The method used consisted of controlled salt saturation, voltages calculated from the electrokinetic properties of each material, and sequential tracking of moisture and soluble salts. Thus, the study intended to provide technical evidence in support of electro-osmosis as a sustainable, non-destructive, and reproducible method for protecting, retaining, and increasing the durability of masonry buildings against the coastal environment.

3. Materials and Methods

3.1. Study Area

Punta Hermosa, located south of Lima, is a coastal district assailed by adverse environmental conditions such as high relative humidity, constant fog, and salt-bearing winds from the sea [27]. This combination promotes corrosion and deterioration of construction materials, which can lead to lower durability of structures [28]. Moreover, cold, wet winters and warm but also salt-laden summers entail continuous immersion of houses by water and marine agents, which cause their potentially useful life to be cut short if proper construction techniques are not put into practice [29]. The urban front facing the sea and exhibiting houses (washed by waves and salt spray) built on permeable soils at risk of early degradation is an essential area to assess solutions for moisture protection, illustrated in Figure 2.

Fig. 2 Study Area

3.2. Construction Characteristics

Regarding the construction system in Punta Hermosa, masonry is predominantly used with 83% of housing shares, followed by reinforced concrete accounting for about 10.2%, timber 1.9%, and finally, reinforced concrete shear walls only occupies 0.9% [10]. showing a clear preference for masonry in the area. The most important indication of moisture in walls is efflorescence, which occurs as a consequence of absorption and diffusion of moisture saturated with soluble salts from the soil, mortar, or bricks themselves. The water rises thanks to capillary action, being expelled on the surface and leaving crystallized deposits that lead to aesthetic damage, detachment of finishes, progressive deterioration of the material, and less useful life for the building. This perennial behaviour compromises the structural integrity and needs regular repair [30, 31]. Rising damp is visible in Figure 3, through the lower area of a residential wall by capillarity and the appearance of finishes and building materials degradation.

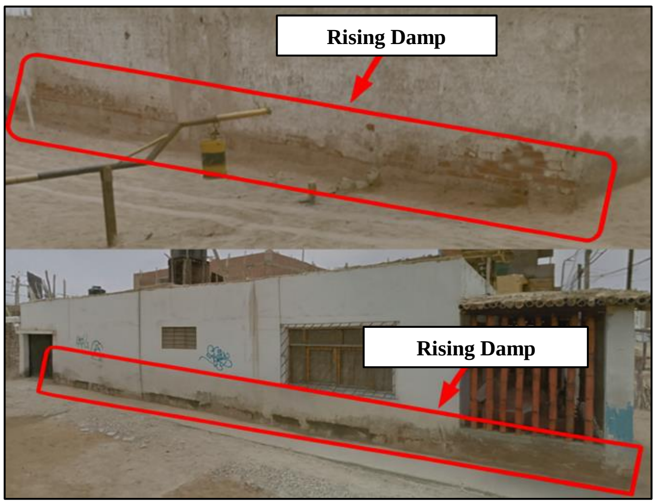

Fig. 3 Humidity in study area

3.3. Materials used in Walls

In this regard, the most representative bricks in the national construction sector are mentioned as pandereta, 18-hole King Kong, solid clay, and concrete block [12]. The materials chosen were selected according to their usual use in masonry housing and with respect to humidity situations and the behaviour of these materials by electro-osmotic treatment.

3.3.1. Pandereta Brick "LP"

Pandereta is a fired clay masonry unit, thin and lightweight in nature, which makes it easy to handle and light so as to be cost-effective for partition walls and enclosures. Based on its geometric configuration and the existence of longitudinal perforations, it guarantees an acceptable thermal and acoustic insulation performance; however, since this material does not have mechanical properties to resist structural loads, it is limited to non-structural components in buildings [32-34]. This research used Pirámide brand pandereta bricks (Figure 4), free from impurities, fired in clay, and polished through quality control processes. The measurements were 23 × 11 × 9 cm, with a mean weight of approximately 2.2 kg, water absorption records lower than 22%, and void ratio values smaller than 57%. They also provided an apparent density of 2.1 g/cm³ and a maximum warpage of 4 mm [35].

Fig. 4 Pyramid Pandereta Brick

3.3.2. King Kong 18-hole Brick with 30% Voids "LKK."

The King Kong 18-hole brick is a type of masonry material prepared from fired clay and characterised by longitudinal perforations that decrease its density while optimising its performance related to heat and acoustic insulation without losing compressive strength [13, 36, 37]. Nevertheless, this sort of brick varies in its dimensions as well as properties to isolate, depending on the design engineer. The King Kong 30% bricks of Pirámide brand, shown in Figure 5, were chosen as they presented the features that provide reliable structural behavior for the purposes of this research. This product had a format of 24 × 13 × 9 cm, manufactured with clay free of impurities and subjected to controlled firing processes, which guaranteed uniformity in its physical and mechanical properties. These included an average weight of 4.1 kg, water absorption of less than 22%, a void area of less than 30%, an apparent density of 2.1 g/cm³, and a compressive strength of more than 180 kg/cm², verified in the laboratory [38-40]. These specifications are in accordance with Technical Standard E.070 on Masonry, which regulates the quality and performance parameters required for use in buildings [41].

Fig. 5 King Kong brick with 18 holes Pyramid

3.3.3. Concrete Brick "LC"

Concrete brick is a prefabricated masonry material made from a mixture of cement, fine and coarse aggregates, and water, which is usually moulded into a hollow shape to reduce its own weight and improve thermal and acoustic performance. Concrete blocks are characterised by their low cost, ease of production, and versatility of use, and are widely used in developing countries for load-bearing and non-load-bearing walls, as well as offering acoustic insulation and fire protection [42-44]. In this research, Pacasmayo B14 concrete blocks, shown in Figure 6, were used, selected for their wide availability in the local market. It is a masonry unit made from cement, water, aggregates, and additives, with a prismatic geometry and modular dimensions of 39 × 14 × 19 cm. This block has a minimum wall thickness of 2.5 cm and achieves an average compressive strength of 7 MPa (71.4 kg/cm²). Its most common applications include load-bearing walls, reinforced masonry systems, perimeter fences, and partitions. It also stands out for offering greater performance on site, reducing construction times and mortar consumption, as well as providing superior durability compared to conventional bricks [45].

Fig. 6 Pacasmayo B14 concrete block

3.3.4. Solid brick "LM"

Solid clay bricks are traditional masonry units made from fired clay without perforations. They are characterised by their compactness, uniform strength, and high water absorption. These properties make them suitable for load-bearing walls in historic and contemporary buildings, although their mechanical behaviour depends both on their moisture content and the type of mortar used in the joint [46, 47]. In this research, King Kong solid bricks were used, as shown in Figure 7. These are fired clay masonry units with a prismatic shape and dimensions of 21 × 9 × 12 cm, weighing approximately 4.1 kg. Because of its high density and strength, this type of brick is used in load-bearing walls, foundations, and in structures subjected to large vertical elements, providing safety and durability to mass buildings [48].

Fig. 7 Solid brick

3.4. Electro-Osmosis

Electro-osmosis is a physical-chemical process in which water movement is generated within porous materials by applying a direct electric current [20, 49]. When electrodes are placed in the damp structure and in the ground, the induced electric field causes the water molecules contained in the capillaries to move from the anode to the cathode, reducing the internal humidity [50]. This phenomenon is based on the interaction between the solid surface of the material and the water in its pores, and allows capillary rise to be controlled or reduced, thereby limiting damage associated with salts, loss of strength, and deterioration of coatings [26]. This process can be seen in Figure 8.

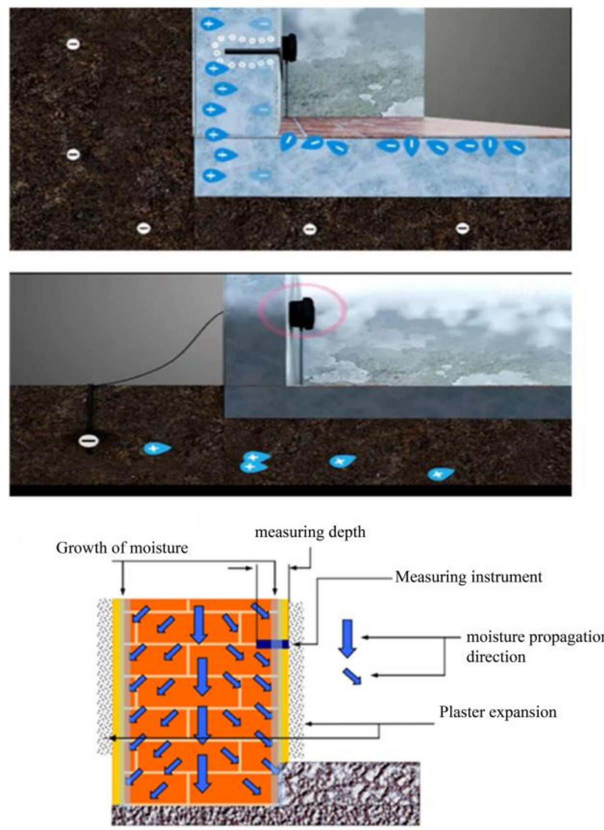

Fig. 8 Electro-osmosis process [21]

3.4.1. Electric Field

The effectiveness of the electro-osmotic process depends mostly on voltage, current density, and material resistivity. Past studies showed that the interplay of these factors, along with the chemical composition and microstructure of the substrate, determined the level of induced water flow, and therefore the efficiency of drying. Electrical continuity and proper placement of the electrodes were also identified as critical conditions for stable and ongoing water migration over time [25, 51]. Based on these electrical criteria and the established theoretical voltage range, the calculation parameters used in this research were defined. To determine the voltage required in the tests, the Helmholtz-Smoluchowski equation (1) was applied, which establishes that electro-osmotic mobility results from the relationship between the dielectric permittivity of water, the zeta potential of the pore surface, and the dynamic viscosity of water [52].

$$\mu eo = \frac{\varepsilon * \zeta}{\eta} \quad (1)$$

The dielectric permittivity of water (ε) used in the calculations was determined considering the test temperature, set at 15 °C, as shown in Figure 9. Based on the values reported in the literature for this condition, an absolute permittivity of 7.43×10^{-10} C/V·m was obtained [53]. Likewise, the zeta potential of the pore surface (ζ) was assigned according to the type of brick analysed: for the pandereta brick, ζ = -0.035 V was adopted; for the 18-hole King Kong brick, ζ = -0.056 V; and for the solid brick, ζ = -0.086 V, values consistent with the behaviour of fired clays of different densities; in the case of concrete brick, as it corresponds to a cementitious matrix, the reported experimental value of ζ = +0.005 V was used [54]. Finally, the dynamic viscosity of water (η) was established based on the same temperature (15 °C), with a value of 1.14×10^{-3} Kg/(m·s), in accordance with the specialist literature [55].

Fig. 9 Water temperature

Based on these values and considering both the geometry of the walls (height, length, and thickness) and the mass of water to be extracted, depending on the initial humidity and target humidity, the voltages required for different drying intervals (7, 14, 30, 60, 90 days) were calculated, as shown in Table 6. These intervals were chosen in order to establish a defined time frame, since most of the research reviewed on electro-osmosis does not specify clear evaluation horizons, limiting itself to general observations or qualitative results. In this way, the aim was not only to quantify the evolution of moisture and salts in short, medium, and long periods, but also to provide a comparative basis for identifying the optimum point of technical and economic efficiency. This provided a robust quantitative basis that facilitated the estimation of optimal voltages and provided an objective criterion for evaluating the feasibility, efficiency, and scalability of the electro-osmotic method in each type of brick analysed.

3.4.2. Moisture Measurement

For this investigation, the R&D MT18 (digital hygrometer) presented in Figure 10 was used: a resistive moisture monitor developed for applications to wood, paper/cardboard, and building materials like brick, concrete block, or drywall. This device boasts an impressive ±0.5% accuracy, with a measurement history of 0.2% to 24%, capable of measuring the moisture levels in walls and floors, allowing measurements from walking distance away, and keeps your documents organized and accurate on a backlit LCD screen (up to one decimal place: 0.1%). It includes a lightweight and portable design, a data hold function, automatic shut-off after five minutes of non-use, and easy operation with three reading modes based on the material [56, 57].

Fig. 10 R&D MT-18 digital hygrometer

3.4.3. Measurement of Soluble Salts

For this study, total soluble salts were analysed according to NTP 339.152:2015 [58], without differentiating concentrations of specific ions like chlorides or sulphates. This choice was made because, as a result of the experimental design, all walls were saturated with the same solution at equitoxic concentration (0.5 M NaCl). Thus, it provided environmentally homogeneous initial conditions. Since the main purpose of the study is to evaluate moisture decrease promoted by electro-osmosis, an overall quantification of soluble salts methodologically supports identifying trends in reduction related to the process and further compensates for the monitoring by a digital hygrometer.

3.4.4. Implementation of Prototypes for Electro-osmosis Testing

To carry out the experimental process of this research, procedures described in the literature were taken as a reference, where electro-osmosis has been applied both in laboratory samples and in real walls, using electrodes and controlled voltages to induce the displacement of water from the anode to the cathode [19, 20, 21, 59].

Initial Conditions of the Bricks

The materials used for laying walls, specifically bricks and coarse sand aggregate obtained from the Orcotuna quarry, were subjected to a preliminary evaluation before being used in the construction process. The purpose of this verification was to ensure that the inputs did not have characteristics that could alter the planned measurements and negatively influence the development of the research. In the case of bricks, Figure 11 shows the efflorescence test in accordance with ASTM C67 [60], which establishes the partial immersion of the units in distilled water for 7 days with a water level of 30 mm, to assess the possible appearance of crystallised salts on their surface. For coarse aggregate, the guidelines set out in standard NTP 339.152:2015 were followed [58], which regulates tests designed to identify the presence of harmful substances such as salts and organic matter. Finally, the results obtained confirmed that neither the bricks nor the aggregate contained salts or other compounds that could pose a risk to the accuracy of the tests or the durability of the constructed wall.

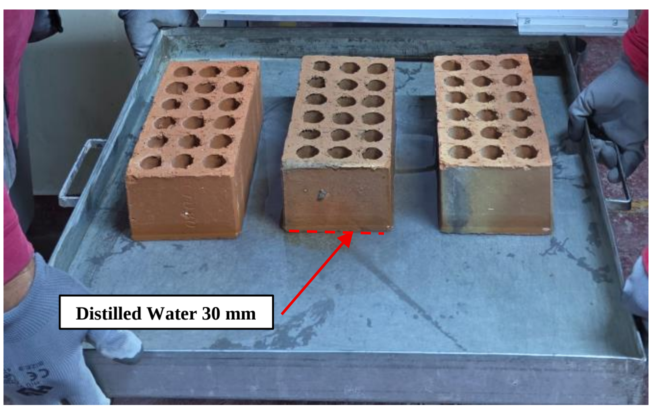

Fig. 11 Efflorescence Test ASTM C67

Construction of Test Walls

Sixty evaluative constructions of adjustable 1.00 m × 1.00 m wall sections were made to ensure the results achieved were repeatable and valid. The dimensions were purposeful, as they would allow for sufficient reproduction of the processes of moisture absorption and transport, and also, they provide a modular unit to extrapolate results to larger-scale walls in real buildings.

The tests corresponded to four types of brick, five application times, and three repetitions for each combination, using pandereta bricks, 18-hole King Kong bricks, concrete blocks, and solid bricks as masonry units, each with its characteristic thickness (0.09 m for the first three and 0.14 m for the concrete block). Prior to laying, all bricks were soaked in clean water for 8 minutes to reduce capillary suction and promote mortar adhesion. The panels were set using a mortar bed created using a 1:5 (cement: coarse sand) ratio, using just enough water to make a mix that could work, and set so it would stick to the panels and provide adequate strength to the joints. Mortar was applied to the panels, and it was set to 1.5 cm, both horizontally and vertically, and the rows were carefully spaced from one another, as shown in Figure 12.

Additionally, the panels were kept moist at average intervals of 12 hours in order to avoid the formation of unidirectional microfractures in the mortar and thus were cured for a period of 7 days [38].

Fig. 12 Bricklaying

Drying the Walls

Once the walls were completed with the curing process, they were left to dry with exposure to natural, fresh air, while being protected from rain. The walls were monitored by means of a hygrometer, from which measurements were taken intermittently at nine predetermined spots on the surface of each panel. These nine spots were divided across three horizontal areas and three vertical heights (0.20 m, 0.50 m, and 0.80 m). To ensure adequate contact between the metal tips of the instrument and the internal material, controlled perforations were made at each measurement point using an electric drill and a 6 mm diameter drill bit, reaching a depth of 15 mm, to guarantee results that were more representative of the actual humidity of the wall.

Measurements were taken every 48 hours to ensure continuous monitoring of humidity changes. On average, the walls reached the reference condition of 'dry' within a period of 30 days, since for bricks and concrete blocks, a moisture content of approximately 2.0% to 2.5% is assumed to be dry [16]; However, the stability criterion was established when the variations recorded were less than 2.5%. This is shown in Figure 13.

Fig. 13 Drying brick walls

Initial Wall Properties

Table 1 shows the density results for walls built with different types of bricks used in the research. To do this, 1 m × 1 m walls with the thickness corresponding to each unit were weighed to determine their total mass, and from this, the density was calculated by dividing by the volume of the wall. Thus, the Pandereta brick wall had a density of 1018 kg/m³ with a mass of 91.62 kg, the 18-hole King Kong brick wall had a density of 1478 kg/m³ with 133.02 kg, the concrete brick wall obtained 1490 kg/m³ with 208.6 kg, and finally, the solid brick wall showed the highest density with 1750 kg/m³ and a mass of 157.5 kg. These results reflected the influence of the type of brick, forming the basis for calculating the theoretical voltage to be applied in each case.

Table 1. Wall density

Type	Thickness (m)	Wall volume (m³)	Wall mass (kg)	Wall density (kg/m³)
LP	0.09	0.09	91.62	1018
LKK	0.09	0.09	133.02	1478
LC	0.14	0.14	208.6	1490
LM	0.09	0.09	157.5	1750

Capillary Saturation Process in Walls

Once the reference dry condition was achieved, the cloths were subjected to a controlled saturation process in order to reproduce an environment similar to that of walls affected by rising damp, as shown in Figure 14. To do this, a perimeter fence was constructed from 18 mm thick plywood, 0.20 m high, enclosing an area of 1.20 × 0.4 m. The fence was secured with screws and dowels spaced every 30 cm to ensure its stability. An in situ 0.5M sodium chloride (NaCl) solution was poured inside the fence, made by dissolving 29.22 g of salt per litre of distilled water (Item a). Therefore, the volume added was a 10 cm high liquid film, allowing contact of its base to the masonry (Item b). As prescribed by ASTM C67, saturation was held over a period of 7 days for overall capillary rise along the wall section [60].

After this period, the excess solution was removed, and each wall was allowed to stabilize for two hours (in order to ensure uniform conditions prior to taking the initial measurements). The application of this saturation procedure created the necessary initial conditions for conducting two complementary tests: measuring the water content of the walls and calculating the soluble salts transported by capillary action.

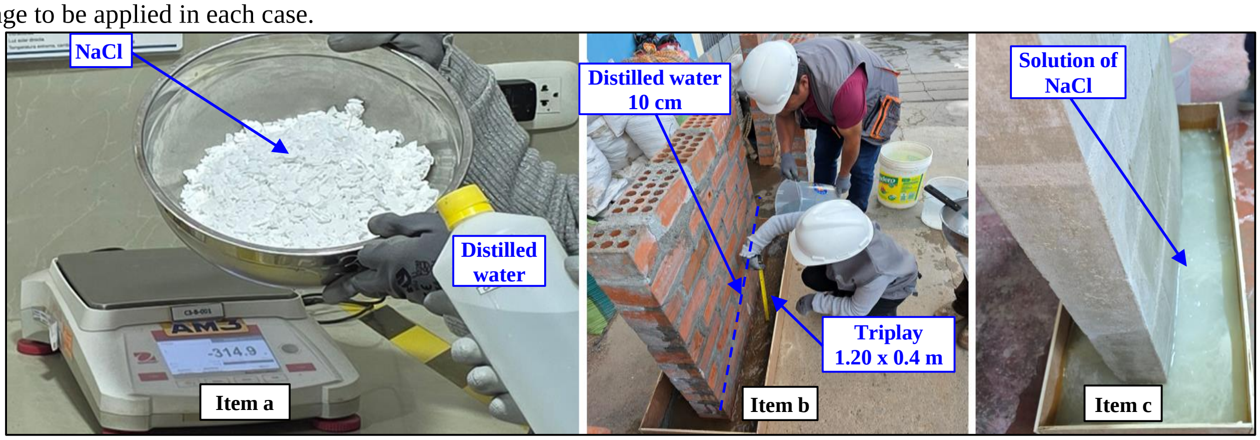

Fig. 14 Saturation of brick walls

Initial Moisture Measurement (Day 0)

The first moisture measurement at saturation, with saline solution, before the two-hour stabilizing time to homogenize the conditions in the wall, and to obtain a mean value of the moisture content over each section evaluated, the measurements were taken with a portable precision hygrometer at three heights in each brick panel (0.20 m, 0.50 m, and 0.80 m). Initial Measurement Process for Test Panels (shown in Figure 15). The reference record (day 0) was these readings, which were used to compare with the evolution of moisture as a factor of corresponding days, as shown in Table 7. The results obtained at this stage are presented in Table 2, forming the baseline for comparison with successive measurements and with the analysis of soluble salts.

Fig. 15 Initial moisture measurement

Table 2. Initial moisture content (%) of walls

Type of Brick	Initial moisture content of test wall after 7 days (%)	Initial moisture content of test wall after 14 days (%)	Initial moisture content of test wall after 30 days (%)	Initial moisture content of test wall after 60 days (%)	Initial moisture content of test wall at 90 days (%)
LP	12.34%	12.36%	12.57%	11.54%	12.85%
LKK	13.26%	12.71%	13.85%	12.50%	13.61%
LC	7.32%	6.81%	7.56%	6.62%	7.42%
LM	11.50%	10.96%	11.85%	10.65%	11.62%

Based on initial moisture measurements of the walls, a target moisture content of 2.50% was established, considered optimal according to previous research to ensure the hygroscopic balance of the masonry and minimize the risks of deterioration due to salts and loss of strength [49, 61]. To determine the mass of water associated with this drying process, the difference between the initial moisture content and the target moisture content was calculated and multiplied by the density and volume of each wall. The results obtained are presented in Table 3, which quantifies the amount of water that had to be removed from each type of brick to achieve the proposed condition.

Table 3. Initial water mass

Prototypes - 7-day trial			
Type of Brick	**Initial wall moisture (%)**	**Desired humidity (%)**	**Δ Water mass (kg)**
LP	12.34%	2.50%	9.020
LKK	13.26%	2.50%	14.310
LC	7.32%	2.50%	10.063
LM	11.50%	2.50%	14.173
Prototypes - 14-day trial			
Type of Brick	**Initial wall moisture (%)**	**Desired humidity (%)**	**Δ Water mass (kg)**
LP	12.36%	2.50%	9.032
LKK	12.71%	2.50%	13.583
LC	6.81%	2.50%	8.993
LM	10.96%	2.50%	13.320
Prototypes - 30-day trial			
Type of Brick	**Initial wall moisture (%)**	**Desired humidity (%)**	**Δ Water mass (kg)**
LP	12.57%	2.50%	9.224
LKK	13.85%	2.50%	15.096
LC	7.56%	2.50%	10.547
LM	11.85%	2.50%	14.723
Prototypes - 60-day trial			
Type of Brick	**Initial wall moisture (%)**	**Desired humidity (%)**	**Δ Water mass (kg)**
LP	11.54%	2.50%	8.281
LKK	12.50%	2.50%	13.301
LC	6.62%	2.50%	8.592
LM	10.65%	2.50%	12.832
Prototypes - 90-day trial			
Type of Brick	**Initial wall moisture (%)**	**Desired humidity (%)**	**Δ Water mass (kg)**
LP	12.85%	2.50%	9.483
LKK	13.61%	2.50%	14.780
LC	7.42%	2.50%	10.259
LM	11.62%	2.50%	14.357

3.4.5. Measurement of Soluble Salts (Day 0)

The determination of total soluble salts was carried out by adapting NTP 339.152:2015 [58], originally applied to soils, to brick dust samples obtained by scraping the surface of walls, structuring the procedure into four main stages: sampling, extract preparation, evaporation and drying, as shown in Figure 16. Item a, in the sampling stage, three reference heights different from those used in moisture measurement (0.20 m, 0.50 m and 0.80 m) were defined for each 1.00 × 1.00 m section, delimiting an area of 20 × 20 mm at each level; Next, the nine points on the wall surface were carefully scraped with a stainless steel spatula to a depth of 5 mm, obtaining 2.50 g of dust per sampling point. Samples were stored in properly labelled airtight polyethylene jars, and dried in an oven at 40 °C for 24 h to ensure the removal of any residual moisture, but without changing the composition of salts. They were cooled in a desiccator and weighed on an analytical balance with a precision of 0.001 g before being analyzed. During the preparation of extract, item b, 2.00 g of dry brick powder was weighed and placed in a 250 mL Erlenmeyer flask followed by addition with distilled water to get a Solid-Water Ratio (S/W) =1:5 depending on standard; The suspension was stirred by use of magnetic stirrer for 60 minutes at rotations per minute, if not otherwise stated, speed then allowed to stand for another 60 minutes at room temperature (20 °C). c was obtained after holding and filtering through a 110mm Büchner funnel with Whatman 934-AH microfibre paper, allowing the collection of an aqueous extract that is truly transparent. Item d, in the evaporation and drying stage, 100 mL porcelain capsules were used, previously conditioned in an oven at 180 °C for one hour, cooled in a desiccator, and weighed on an analytical balance to record the initial mass (m_1); an aliquot of 10.0 mL of the filtrate obtained was poured into each capsule. Item e, finally, the capsules were dried in an oven at 180 °C for one hour, cooled in a desiccator, and weighed again to record the final mass (m_2). Finally, in the calculation and expression of results stage, the total soluble salt content was obtained using Equation (2), as defined in NTP 339.152:

$$SS(mg/kg) = \frac{(m1-m2)\times D\times 10^6}{E} \quad (2)$$

Where (m1 - m2) corresponds to the increase in mass in grams due to salt residue, D = 5 is the solid-water ratio used, and E = 10 mL is the volume of the evaporated filtrate. Thus, the result was expressed in milligrams of soluble salts per kilogram of dry brick (mg/kg), a unit equivalent to parts per million (ppm).

Fig. 16 Procedure for measuring soluble salts

For interpretation, the ranges established in standard UNE-EN 771-1:2011+A1:2016 were used, which classify the soluble salt content into categories S0, S1, and S2 based on the maximum percentage by mass of soluble ions [62]. This classification is shown in Table 4. It should be noted that Peru does not yet have specific regulations governing this parameter in bricks, which is why the international reference was used as a technical framework for comparison and evaluation of the risk of efflorescence.

Table 4. Soluble salt ranges

Category	Maximum mass content	Equivalent (mg/kg)	Associated risk
S2	$Na^+ + K^+ \leq 0.06\%$ y $Mg^{2+} \leq 0.03\%$	≤ 600 mg/kg	Very low [58]
S1	$Na^+ + K^+ \leq 0.17\%$ y $Mg^{2+} \leq 0.08\%$	≤ 1700 mg/kg	Moderate [58]
S0	No specific requirement	> 1700 mg/kg	High [63]

Table 5 shows that most of the wall prototypes exceeded the threshold of 1700 mg/kg established by the UNE-EN 771-1:2011+A1:2016 standard, corresponding to category S0 (high salt content). The walls built with pandereta bricks recorded values between 2000 and 2150 mg/kg, remaining consistently high. The prototypes with 18-hole King Kong bricks achieved the highest values, with a maximum of 2300 mg/kg, which shows their greater susceptibility to efflorescence.

Concrete block walls, on the other hand, showed different behaviour: although the prototypes prepared for 30 days were in the high category (1750 to 1850 mg/kg), those prepared for 60 and 90 days fell to 1600 and 1700 mg/kg, moving into the S1 (moderate) category. Finally, solid brick walls reached up to 1980 mg/kg, remaining in the high salt content category throughout the period. These results confirm that the saline solution applied to the prototypes generated the presence of soluble salts in the walls, successfully reproducing critical conditions for efflorescence risk.

Table 5. Initial soluble salts (day 0)

Pandereta Brick "LP"					
Days	**7 days**	**14 days**	**30 days**	**60 days**	**90 days**
m_1 (g)	48.5372	48.7653	49.1096	49.0024	49.2801
m_2 (g)	48.5331	48.7611	49.1055	48.9981	49.2761
SS(mg/kg)	2050	2100	2050	2150	2000
Classification	High	High	High	High	High
King Kong 18-hole brick "LKK."					
Days	**7 days**	**14 days**	**30 days**	**60 days**	**90 days**
m_1 (g)	46.1331	46.5066	46.9057	46.2368	46.7832
m_2 (g)	46.1287	46.5021	46.9011	46.2324	46.7789
SS(mg/kg)	2200	2250	2300	2200	2150
Classification	High	High	High	High	High
Concrete block "LC."					
Days	**7 days**	**14 days**	**30 days**	**60 days**	**90 days**
m_1 (g)	47.5558	47.1027	47.8936	47.3343	47.7435
m_2 (g)	47.5523	47.0991	47.8899	47.3311	47.7401
SS(mg/kg)	1750	1800	1850	1600	1700
Classification	High	High	High	Moderate	Moderate
Solid brick "LM."					
Days	**7 days**	**14 days**	**30 days**	**60 days**	**90 days**
m_1 (g)	44.9869	45.3163	45.7817	45.0542	45.6159
m_2 (g)	44.9832	45.3124	45.7777	45.0505	45.6123
SS(mg/kg)	1850	1950	1980	1850	1800
Classification	High	High	High	High	High

Installation of the Electro-Osmosis System

After the initial measurements, the electro-osmosis system was installed on the 1.00 × 1.00 m sections. Copper rods (3/4" × 100 mm) were used as anodes, fixed to the wall surface with Thor Cem cement-based conductive mortar, ensuring adequate electrical contact. These electrodes were located 0.80 m above the base and connected to the positive pole of the direct current source. The cathode consisted of a stainless-steel rod 10 mm in diameter and 200 mm in length, buried vertically 10 cm deep in the damp ground next to the base of the wall (Figure 17). This configuration replicated the layout used in real buildings, adapted to the scale of the prototypes. The system was powered by a YIHUA 605D-III adjustable direct current source (0-60 V), which allowed the voltages calculated and recorded in Table 6 to be applied.

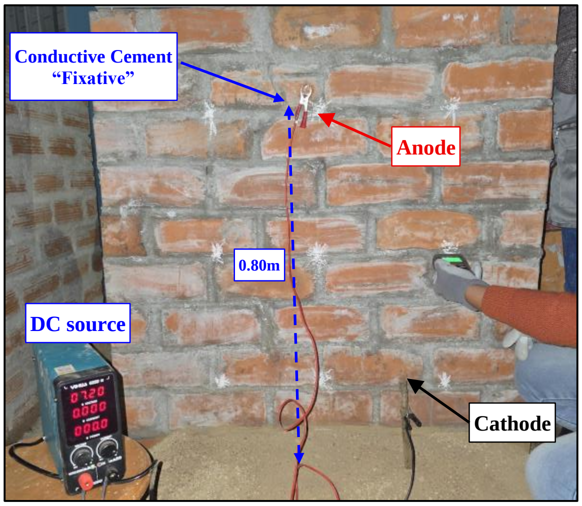

Fig. 17 Installation of the Electro-Osmosis system

The operating voltages were determined based on the physical and electrokinetic properties of each type of brick, with the aim of reducing the initial moisture content of the prototypes to the reference value of 2.50%, considered the optimal hygroscopic condition for ensuring stability and minimising the risk of deterioration [49, 61]. To achieve this objective, the mass of water to be extracted from each wall was calculated in advance (Table 3), obtained from the difference between the initial moisture content measured after salt saturation and the target moisture content, multiplied by the density and volume of each wall prototype. This procedure made it possible to accurately quantify the volume of water that had to migrate under the action of the electric field. After that, taking these values, the wall dimensions (1.00 × 1.00 m and the thickness for each type of brick), as well as the distinct electrokinetic attributes of the materials, the dielectric permittivity of water at 15 °C, the viscosity of water under these conditions, the zeta potential of the brick's surface porosity, and applying the Helmholtz-Smoluchowski equation (Equation 1). This relationship allowed the electro-osmotic mobility to be estimated and, from this, the specific theoretical voltages required to induce water flow towards the cathode. In this way, different voltage ranges were defined for each material and time horizon (7, 14, 30, 60, and 90 days) using Equation 3, ensuring that the energy levels applied were sufficient to achieve the expected dehumidification without compromising the integrity of the walls. In addition, this methodological approach provided a quantitative and replicable criterion, which not only allowed for the comparison of the behaviour of different types of brick, but also for the evaluation of the practical feasibility and energy efficiency of the electro-osmotic method as a technique for the conservation of homes in coastal areas.

$$Vtheorical = \frac{\Delta M * d}{\mu eo * A * t} \quad (3)$$

Where: (ΔM) is the mass of water in m³, (d) is the distance between the anode and electrode in m, (μeo) is the reference mobility in m²/V.s, (A) is the contact surface area in m², and t is the time in min.

Table 6. Theoretical voltage applied to brick walls

Brick Type	Volts (V) for 7 days	Volts (V) for 14 days	Volts (V) for 30 days	Volts (V) for 60 days	Volts (V) for 90 Days
Pandereta Brick "LP"	7.264	3.637	1.733	0.778	0.594
King Kong 18-hole Brick "LKK."	7.203	3.419	1.773	0.781	0.579
Concrete Brick "LC"	36.472	16.296	8.919	3.633	2.892
Solid Brick "LM"	4.645	2.183	1.126	0.491	0.366

According to the theoretical application quantities, it was observed that the highest calculated voltage was 36.47 V, a value that is below the 50 V limit established by the Occupational Safety and Health Administration (OSHA) as the voltage at which energised parts must be protected because they pose a risk of direct electrical contact [64]. This ensured that potential levels applied to the walls did not exceed those which would be regarded as acceptable for human handling during the electro-osmosis test, thereby avoiding any risk of shock or surface conduction in wet materials.

Humidity Monitoring

For the control of moisture in the walls, points were distributed taking into account a methodology applied in reference studies, with horizontal and vertical spacing [20, 59]. For each 1.00 × 1.00 m area, nine horizontal positions were determined on the surface, and measurements were made at three reference heights, 0.20 m, 0.50 m, and 0.80 m with an effective depth of 10 mm in the masonry (Figure 18) using a digital contact hygrometer.

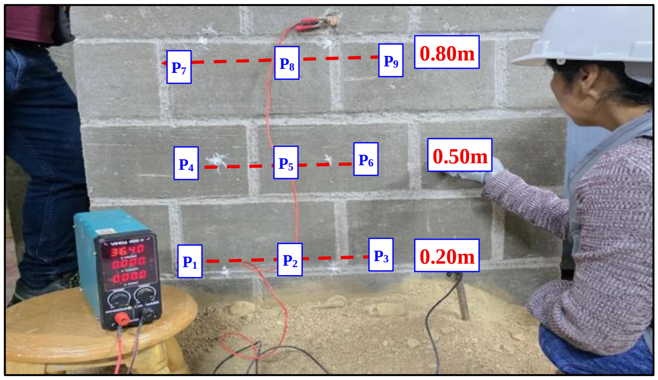

Fig. 18 Humidity monitoring

To ensure more precise control of the dehumidification process and verify stability after the theoretical drying time, an additional measurement equivalent to the established monitoring frequency was considered for each period, which confirmed the trend of moisture reduction. The detailed schedule is presented in Table 7.

Table 7. Humidity monitoring

Theoretical deadline	Measurement frequency	Monitoring days (including additional)
7 days	Daily	Day 1, Day 2, Day 3, Day 4, Day 5, Day 6, Day 7, Day 8
14 days	Every 2 days	Day 1, Day 3, Day 5, Day 7, Day 9, Day 11, Day 13, Day 14, Day 16
30 days	Every 3 days	Day 1, Day 4, Day 7, Day 10, Day 13, Day 16, Day 19, Day 22, Day 25, Day 28, Day 30, Day 33
60 days	Twice a week	Day 1, Day 5, Day 9, Day 13, Day 17, Day 21, Day 25, Day 29, Day 33, Day 37, Day 41, Day 45, Day 49, Day 53, Day 57, Day 60, Day 64
90 days	Weekly	Day 1, Day 8, Day 15, Day 22, Day 29, Day 36, Day 43, Day 50, Day 57, Day 64, Day 71, Day 78, Day 85, Day 90, Day 97

Monitoring of Soluble Salts

So while moisture was monitored in parallel, control of soluble salts on wall prototypes was achieved, but at far larger intervals between measurements. For instance, the nature of crystallised salts progressively evolves in time at large because it is related to the phenomenon processes of ion migration, crystallisation, and puffed up on the surface, as opposed to moisture monitoring, where frequent readings are required because moisture exhibits rapid variations. The monitoring is shown in Table 8.

Table 8. Monitoring of soluble salts

Theoretical deadline	Measurement Frequency	Monitoring Days
7 days	3 times	Day 0, Day 3, Day 7
14 days	3 times	Day 0, Day 7, Day 14
30 days	3 times	Day 0, Day 15, Day 30
60 days	3 times	Day 0, Day 30, Day 60
90 days	3 times	Day 0, Day 45, Day 90

Thus, only five representative time point measurements were planned (7, 14, 30, 60, and 90 days), which allowed for the detection of major changes without performing daily monitoring. The salt vapour method is only because the value for changing from base materials to salts requires an invasive type method (surface scratching of the heart), which can compromise the integrity of walls if too frequent. Thus, the schedule aimed to regulate the collection of reliable data against repercussions in preserving the prototypes themselves, preventing changes in their physical properties while reproducing in a controlled manner comparable events triggering the risk of efflorescence. The sampling of salt was also distributed in a manner dissimilar to that used for moisture, given the intrusive nature of the technique and the effort to reduce disturbance of material within control areas. The spatial arrangement adopted is shown in Figure 19, which shows the location of the extraction points used specifically for the quantification of salts.

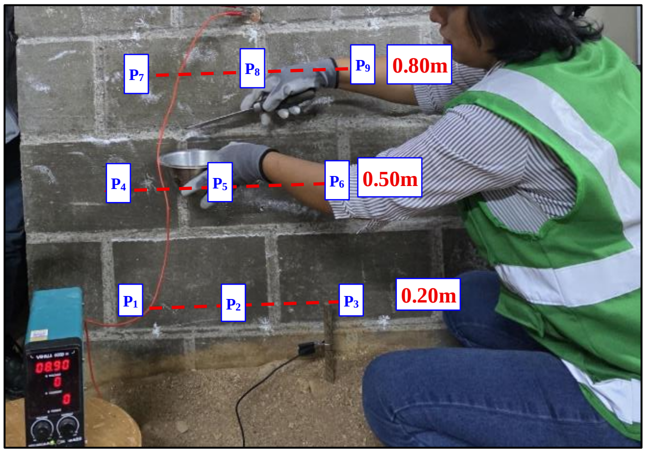

Fig. 19 Salt monitoring

4. Results

This section presents the results obtained from experimental tests carried out on walls built with pandereta bricks, 18-hole King Kong bricks, solid bricks, and concrete blocks. It shows the variations in moisture content recorded during the different application intervals (7, 14, 30, 60, and 90 days), as well as the evolution of the concentration of crystallised salts on the surface of the walls. The estimated costs of implementing the electro-osmosis system are also included, based on the operating time, considering the energy consumption associated with the applied voltages and the replacement of the electrodes.

4.1. Control of 7-Day Prototypes

The results from monitoring moisture and salts at each stage are presented below in Tables 9 and 10, respectively.

4.1.1. Moisture in 7-Day Prototypes

Table 9 shows that all materials reached moisture values close to the reference threshold (2.5%) after eight days of application, although with particular behaviours. The initial moisture content of the pandereta brick was at 12.345% and was reduced to 2.471%, demonstrating the effective drying and rapid water loss due to the porosity of the sample and the applied voltage of 7.264 V. The starting value of the King

Kong brick was the highest at 13.258%, and it also reduced its moisture content to 2.463%. This demonstrated the progressive drying attributed to the compactness of the sample and also the presence of perforations that aided water migration at almost the same voltage (7.203 V). This solid brick started at 11.499% and reduced to 2.461% with a considerable moisture loss, and even though there was the greatest density with no perforations, it still demonstrated that at 4.645 V, electro-osmosis was still effective. The concrete brick had the lowest starting value at 7.324% and, with a required highest operating voltage of 36.472 V, reduced its moisture content to 2.487%. This confirmed that the sample required more energy to induce water flow due to the cementitious matrix and lower porosity. In conclusion, while all the materials had different starting conditions and resulted in different electric settings, it was observed that they all had the same moisture reduction within the set operational time, validating the electro-osmosis techniques.

Table 9. Moisture monitoring of 7-day prototypes

Type of Brick	Monitoring of prototypes for 7 days + 1 check-ups / Daily									
	Theoretical voltage (V)	Humidity (%)								
		Day 0	Day 1	Day 2	Day 3	Day 4	Day 5	Day 6	Day 7	Day 8
LP	7.264	12.345	9.556	7.078	5.124	3.841	3.074	2.685	2.511	2.471
LKK	7.203	13.258	9.131	6.634	4.851	3.877	3.114	2.675	2.486	2.463
LC	36.472	7.324	5.811	4.784	4.036	3.458	3.054	2.716	2.491	2.487
LM	4.645	11.499	7.813	5.774	4.515	3.698	3.141	2.762	2.494	2.461

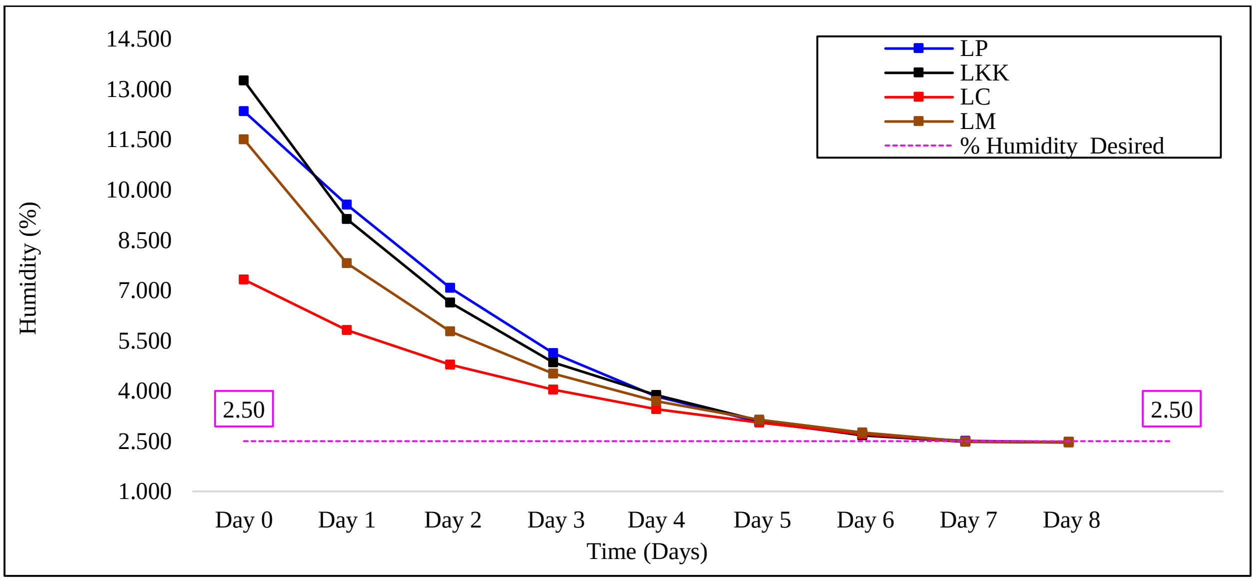

Fig. 20 Humidity monitoring 7-day prototypes

Figure 20 illustrates four distinct drying patterns. Overall, during the first three days, a uniform downward trend in moisture content was observed, although the drying rate varied among the different masonry units. The pandereta brick exhibited the greatest reduction at the beginning, suggesting a better efficiency in moisture removal during the initial stages. The King Kong bricks were also observed to undergo a minor deceleration phase, post which the decrease in moisture content was gradual, and after many weeks, very steady due to the fact that their internal perforations enable the carry of water through them. The massive brick experienced the most consistent drop in the first period, exhibiting a homogeneous reaction despite its relatively dense structure. In stark contrast, the concrete block showed a gradual and smoother decay that is controlled by its compact and dense matrix of cement, restricting fluid movement. All materials achieved a moisture content approximately equal to 2.5% by Day 7, which was consistent with an equivalent hygroscopic equilibrium condition governed by voltage regulation conditions. He states that further reduction below this value was not justified since the energy needed for such a process would be high and, at the same time, would contribute relatively little to the extraction of moisture.

Table 10 shows that different types of bricks and different time intervals caused the electro-osmotic process to yield different results. Despite solid bricks recording the highest initial reading of 32.05%, this value gradually decreased to 1.32% by the eighth day. This showed that there is a quick initial response (32.05% the first day), followed by a gradual decrease. King Kong bricks also had a similar response (31.13%), where the leading response decreased to 0.93% in the final interval, not reaching the 20% effectiveness until the fourth day. The pandereta brick showed intermediate behaviour. 22.59% was recorded on the first day, with a maximum of 27.60% on the third day, and decreasing gradually to 1.60%, suggesting that this brick's greatest effectiveness was in the initial phase. The concrete block recorded the lowest solid bricks at 20.66% and decreased to the 0.16% final interval. This confirmed that the concrete brick's matrix was the most dense and limited the magnitude of the electro-osmotic effect with a constant and stable decrease.

Table 10. Monitoring moisture effectiveness on 7-day prototypes

Type of Brick	Efficacy according to time (%) for 7-day prototypes							
	Day 0 - Day 1	Day 1 - Day 2	Day 2 - Day 3	Day 3 - Day 4	Day 4 - Day 5	Day 5 - Day 6	Day 6 - Day 7	Day 7 - Day 8
LP	22.59%	25.93%	27.60%	25.04%	19.97%	12.65%	6.48%	1.60%
LKK	31.13%	27.35%	26.88%	20.08%	19.68%	14.10%	7.07%	0.93%
LC	20.66%	17.67%	15.64%	14.32%	11.68%	11.07%	8.28%	0.16%
LM	32.05%	26.10%	21.80%	18.10%	15.06%	12.07%	9.70%	1.32%

From Figure 21, it can be seen that all efficiency curves exhibit a downward trend towards the eighth day; however, the rate of change for each material is different. Both solid brick and King Kong noticeably had higher initial peaks, which declined more rapidly. The pandereta, on the other hand, had an initial increase until the third day before beginning its decline, which set it apart by demonstrating an intermediate maximum efficiency point. In contrast, the concrete block showed a flatter curve, without marked increases, reflecting sustained but less intense action throughout the test. A notable aspect was that, despite these differences, all curves converged towards values close to zero in the last interval, confirming that the maximum effectiveness of electro-osmosis was concentrated in the first Days and tended to stabilize over time.

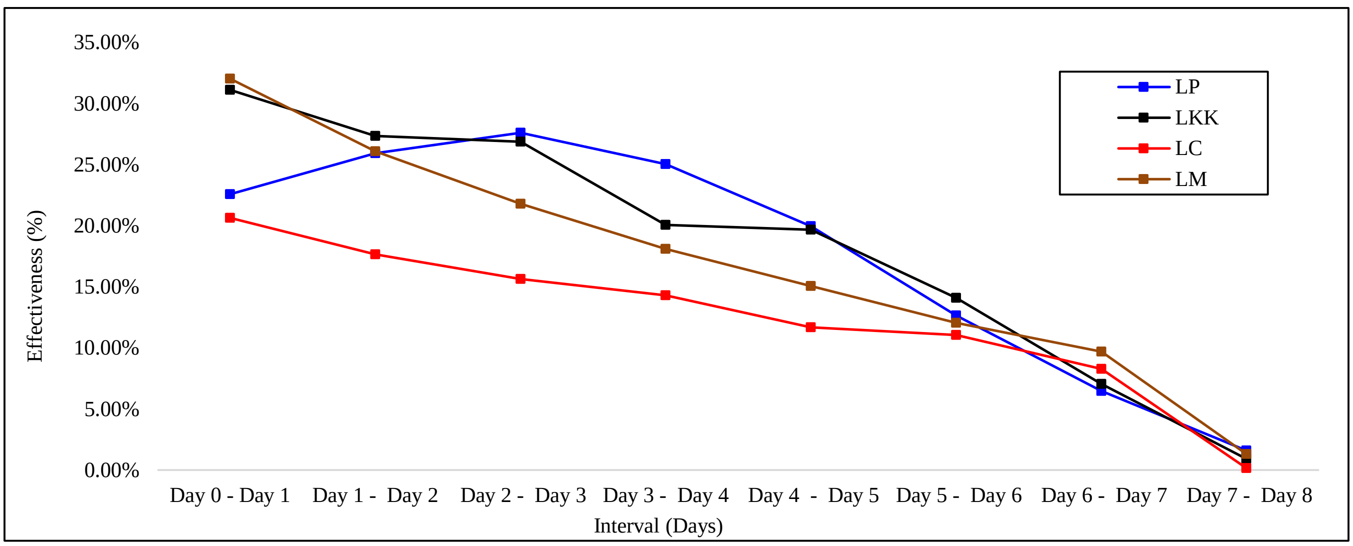

Fig. 21 Moisture effectiveness monitoring - 7 Days

4.1.2. Days Soluble Salts in the 7 Days Prototypes

Table 11 shows the results of applying electro-osmosis for a period of 7 days to the wall prototypes. The pandereta brick (LP) reduced its salt content from 2050 mg/kg to 800 mg/kg, a result attributed to its high porosity and thin geometry, which favoured ion migration under the electric field and also explained its high initial accumulation. The 18-hole King Kong brick (LKK) had the highest initial concentration (2200 mg/kg), decreasing to 750 mg/kg; this behaviour was due to its greater number of voids and capillary connectivity, which makes it very susceptible to salt accumulation, but also highly receptive to treatment. In the case of the concrete block (LC), the values decreased from 1750 mg/kg to 610 mg/kg, a reduction that was achieved by applying a higher voltage that compensated for the lower porosity of the cement matrix and allowed the transport of salts through micro-cracks and interconnected channels. Finally, solid brick (LM) went from 1850 mg/kg to 650 mg/kg, showing a progressive decrease explained by its compactness, which slows down the ion migration process, although the action of the electric field also allowed the salts present in its most accessible pores to be evacuated.

Table 11. Monitoring of soluble salts in 7-day prototypes

Type of Brick	Monitoring of 7-Day Prototypes						
	Theoretical Voltage (V)	SS (mg/kg)				Effectiveness over time	
		Day 0	Day 3	Day 7	Final Condition	Day 0-Day 3	Day 3-Day 7
LP	7.264	2050	1250	800	Moderate	39.02%	36.00%
LKK	7.203	2200	1150	750	Moderate	47.73%	34.78%
LC	36.472	1750	950	610	Moderate	45.71%	35.79%
LM	4.645	1850	1050	650	Moderate	43.24%	38.10%

Figure 22 shows the evolution of the effectiveness of the electro-osmotic process in the wall prototypes during the 7 days of application. In the first interval (Day 0-Day 3), the highest efficiencies were achieved, with values between 39% and 47%, with King Kong brick (47.73%) and concrete block (45.71%) standing out as the materials with the highest initial response. This indicated that, in the first few days, electro-osmosis acted mainly on the most mobile and easily soluble salts, generating a rapid purification effect. In the second section (Day 3-Day 7), the effectiveness decreased slightly to ranges of 34% to 38%, with the solid brick (38.10%) showing the most stable performance. This behaviour showed that, as time progressed, the process faced less accessible salt fractions, trapped in micro-pores or more firmly bound to the material matrix, which slowed down their extraction. Overall, the graph confirmed that electro-osmosis was characterised by an initial phase of high efficiency, followed by a stabilisation stage, maintaining sustained reductions that allowed the risk of efflorescence to be controlled in the different types of brick.

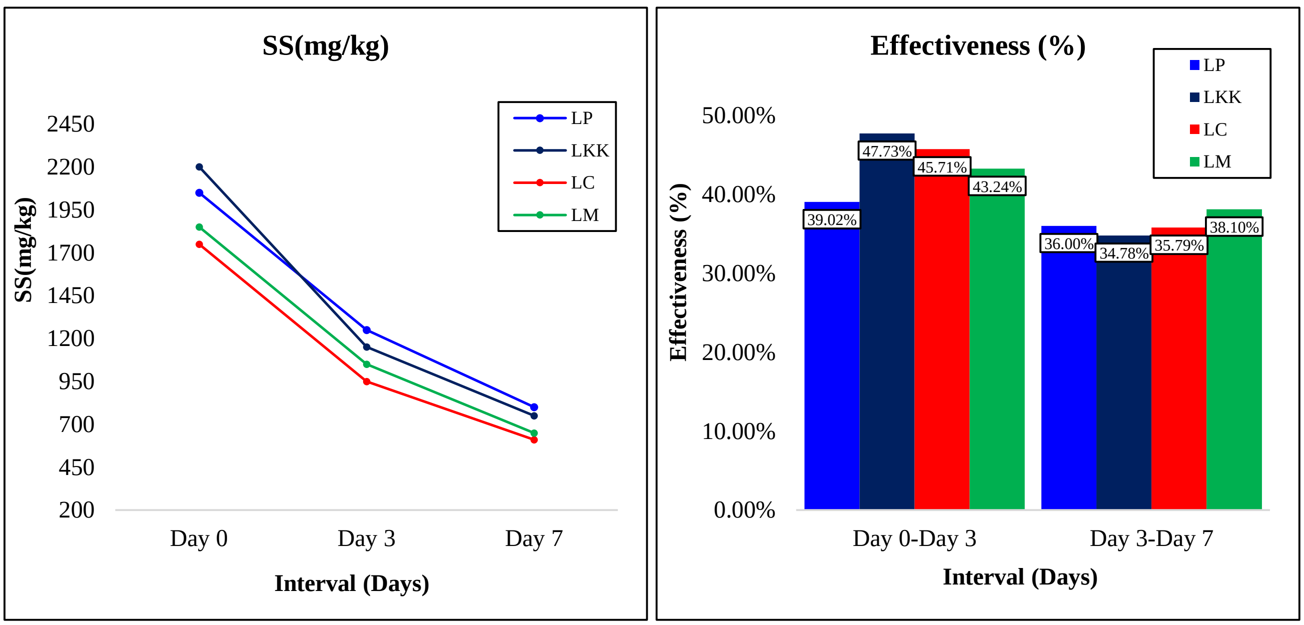

Fig. 22 Soluble salts - 7 days prototypes

4.2. Control of 14-Day Prototypes

4.2.1. Moisture Content of 14-Day Prototypes

All masonry units exhibited a reduction in moisture content, reaching values close to the reference threshold of 2.5% by Day 16, as shown in Table 12. The pandereta brick decreased from 12.359% to 2.491% under an applied voltage of 3.637 V, showing a consistent decline, particularly during Days 1 to 7, when it lost nearly 7 percentage points. In the same manner, the moisture content of King Kong brick was reduced from 12.712% to 2.479%, with a measurable improvement between Days 3 and 7 due to its internal perforated structure, which improved moisture conduction. The solid brick dropped from 10.957% to 2.468%, suggesting it could dry well in spite of its compact structure, using the lowest applied voltage (2.183 V) and sustaining a continuous decrease throughout the record duration period. On the contrary, the concrete block, which had initially shown lower moisture content (6.811%), needed more energy consumption (16.296 V) and got a lower reduction of 2.481%, which sustains growth for drying dense cementitious matrices, which need much more energy to evaporate water into vapor, as well.

Table 12. Moisture monitoring on 14-day prototypes

Type of Brick	Monitoring of Prototypes for 14 Days + 1 control / Every 2 Days										
	Theoretical voltage (V)	Humidity (%)									
		Dia 0	Day 1	Day 3	Day 5	Day 7	Day 9	Day 11	Day 13	Day 14	Day 16
LP	3.637	12.359	9.412	7.181	5.634	4.464	3.671	3.093	2.684	2.511	2.491
LKK	3.419	12.712	8.983	6.674	5.211	4.218	3.511	2.973	2.625	2.491	2.479
LC	16.296	6.811	5.468	4.567	3.882	3.393	3.071	2.814	2.611	2.482	2.481
LM	2.183	10.957	8.512	6.545	4.934	3.913	3.251	2.833	2.581	2.473	2.468

The downward trends for the four brick types in Figure 23 were uniformly aligned, showing steeper slopes in the initial days, which then gradually stabilised as the values approached the target. Pandereta and King Kong bricks exhibited parallel trends, demonstrating accelerated declines until Day 7, and from Day 13 showed convergence towards the reference line. The solid brick displayed an intermediate curve, showing a gradual reduction that remained constant throughout the period. The concrete block, in contrast, showed the lowest curve from the beginning, but with a lower slope reflecting a slower, but continual process until reaching the same final level as the other materials. One converging aspect was that all the trend lines culminated around Day 14, validating that regardless of the material characteristics or the applied voltage, the results of moisture content were standardised due to electro-osmosis at the conclusion of the trial.

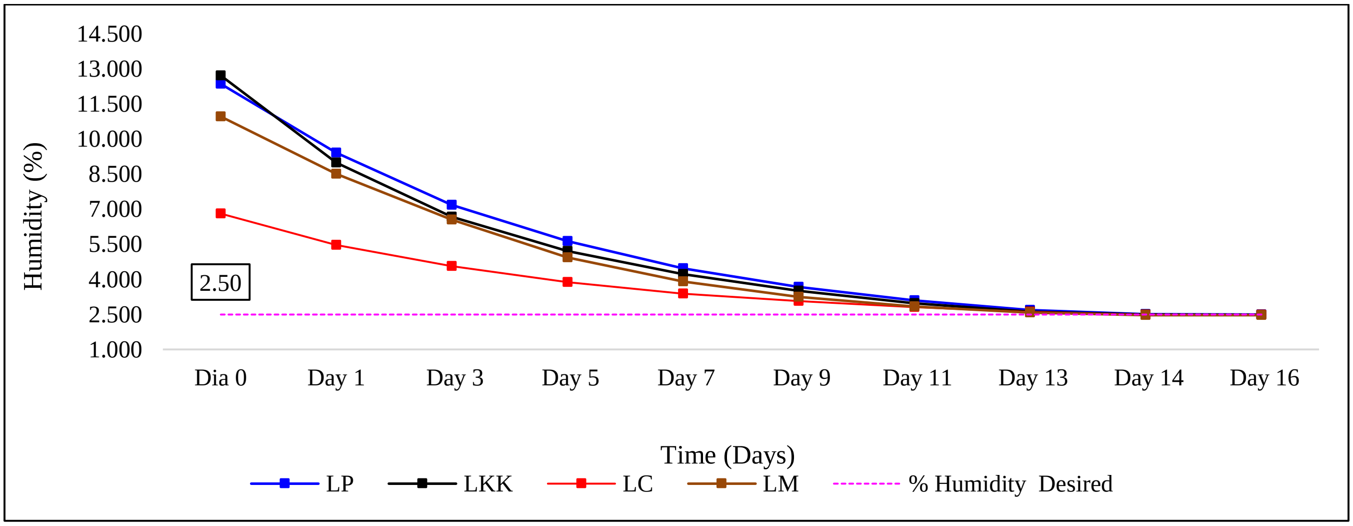

Fig. 23 Humidity monitoring - 14 Days prototypes

As the time intervals progressed, Table 13 shows the decreased effectiveness of electro-osmosis for all materials. With 29.33% entering effectiveness, King Kong Brick recorded the highest value, and for 5 days remained above 20%. Then on Day 16, 0.40% was recorded, which shows strong effectiveness and a significant decline during the last phase. Starting with 23.84%, Pandereta Brick decreased all the way to 0.80% with stable data during the first part of the test and an abrupt decrease during the last days. A unique rebound was recorded for the solid brick on the 3rd interval of 24.61%, then 0.20% was recorded, indicating that, for its compactness, an intermediate performance was kept during the first days. Throughout the test, the lowest efficiency was recorded for the concrete block. With 19.72% starting value, it was recorded up to 0.04%. Also, with a consistent and uniform decrease, it was confirmed that the lower porosity and the higher density limited the response during the test.

Table 13. Monitoring moisture effectiveness on 14-day prototypes

Type of Brick	Efficacy over time (%) at 14-day prototypes								
	Dia 0 - Day 1	Day 1 - Day 3	Day 3 - Day 5	Day 5 - Day 7	Day 7 - Day 9	Day 9 - Day 11	Day 11 - Day 13	Day 13 - Day 14	Day 14 - Day 16
LP	23.84%	23.70%	21.54%	20.77%	17.76%	15.75%	13.22%	6.45%	0.80%
LKK	29.33%	25.70%	21.92%	19.06%	16.76%	15.32%	11.71%	5.10%	0.40%
LC	19.72%	16.48%	15.00%	12.60%	9.49%	8.37%	7.21%	4.94%	0.04%
LM	22.32%	23.11%	24.61%	20.69%	16.92%	12.86%	8.90%	4.18%	0.20%

Figure 24 shows that the efficiency curves generally declined over time, with a notable focus of efficacious activity occurring during the initial seven days, followed by a rapid approach towards ineffective values from the 13th day onwards. The King Kong brick stood out for maintaining the highest curve in the first intervals, followed by the pandereta brick, which showed a more progressive decline. The solid brick differed in its brief initial rise before aligning with the downward trend of the other materials. In contrast, the concrete block showed the lowest and most stable curve throughout the test, with less abrupt declines but also with lower cumulative effectiveness. Overall, the figure showed that, although there were differences in the intensity and shape of the curves, all materials tended to lose effectiveness over time, confirming that the greatest impact of electro-osmosis was concentrated in the initial phase of treatment.

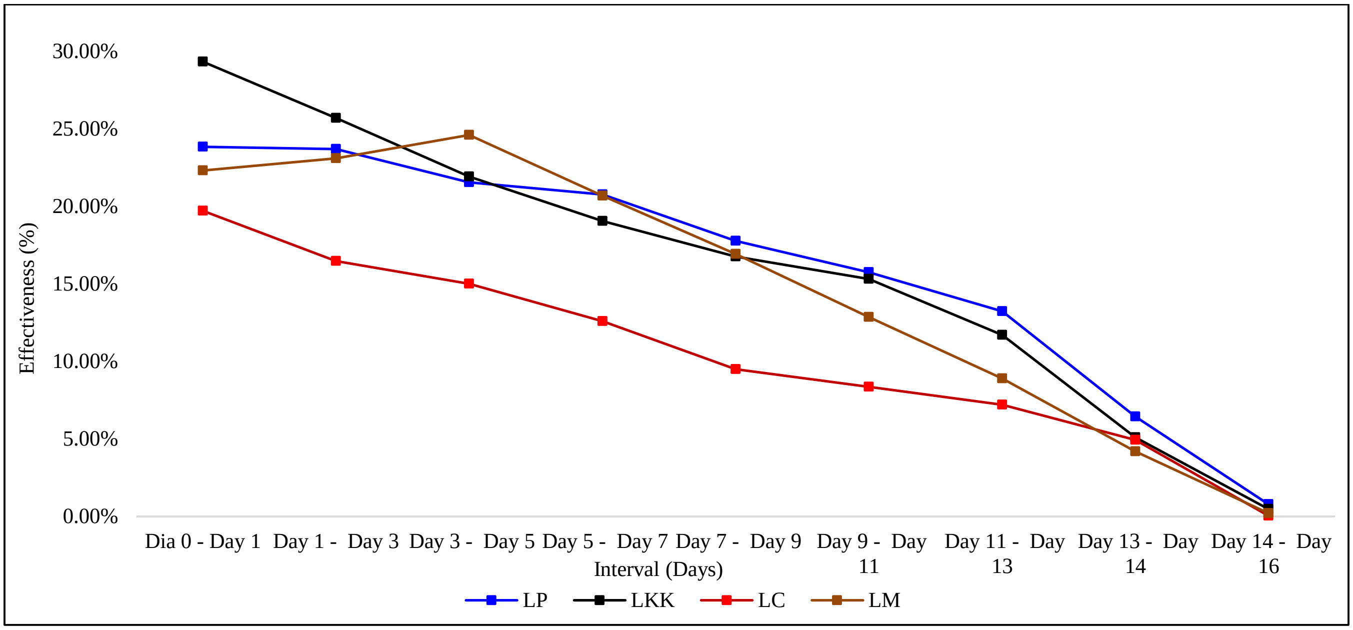

Fig. 24 Salt monitoring, humidity effectiveness monitoring 14-day prototypes

4.2.2. Soluble Salts at 14 Days

Table 14 shows the results of applying electro-osmosis for 14 days to the prototype walls. The pandereta brick (LP) reduced its salt values from 2100 mg/kg to 550 mg/kg, reaching the very low category; this reduction was due to its high porosity, which favoured ion migration and allowed for a more efficient process in the second week of treatment. The 18-hole King Kong brick (LKK), which had the highest initial concentration at 2250 mg/kg, decreased to 590 mg/kg; this result confirmed its high susceptibility to salt accumulation, but also its ability to respond quickly to the electric field thanks to the presence of interconnected capillaries. In the example of the concrete block (LC), the values decreased from 1800 mg/kg to 470 mg/kg. This means that although the block had lesser porosity, the application of a higher voltage (16,296 V) facilitated the movement of salts through the microcracks and gels of the cement matrix. Regarding the solid brick walls (LM), they reduced their concentration from 1950 mg/kg to 500 mg/kg. This means that, although the compactness of the material reduced the speed of ion migration, electro-osmosis was equally effective in removing the salts that had accumulated in the pores of the material. Overall, all of the materials went from a high initial concentration to a very low concentration, and in just two weeks, the process was able to achieve a significant reduction of the risk of efflorescence.

Table 14. Monitoring of soluble salts in 14-day prototypes

Type of Brick	Monitoring of 14-Day Prototypes						
	Theoretical voltage (V)	SS (mg/kg)				Effectiveness over time	
		Day 0	Day 7	Day 14	Final Condition	Day 0-Day 7	Day 7-Day 14
LP	3.637	2100	1240	550	Very low	40.95%	55.65%
LKK	3.419	2250	1140	590	Very low	49.33%	48.25%
LC	16.296	1800	950	470	Very low	47.22%	50.53%
LM	2.183	1950	1080	500	Very low	44.62%	53.70%

Figure 25 illustrates the percentage efficacy achieved during the 14-day evaluation period. During the first interval (Day 0-Day 7), the recorded rates were between 40%-49%, among which King Kong brick was the leading performer with 49.33%, followed by the concrete block with 47.22%. In the subsequent interval (Day 7-Day 14), all recorded rates in the sample exceeded 50%, with pandereta brick and solid brick having the greatest performance at 55.65% and 53.70%, respectively. This trend indicated that following the first week, when the most soluble salts were removed, the system continued to purify more tightly bound salts within the pores, demonstrating ascending efficacy. The graph thus confirmed that electro-osmosis was not only effective in the initial stage, but also exhibited sustained removal capacity in the following days, ensuring a progressive decrease in salts in all wall types evaluated.

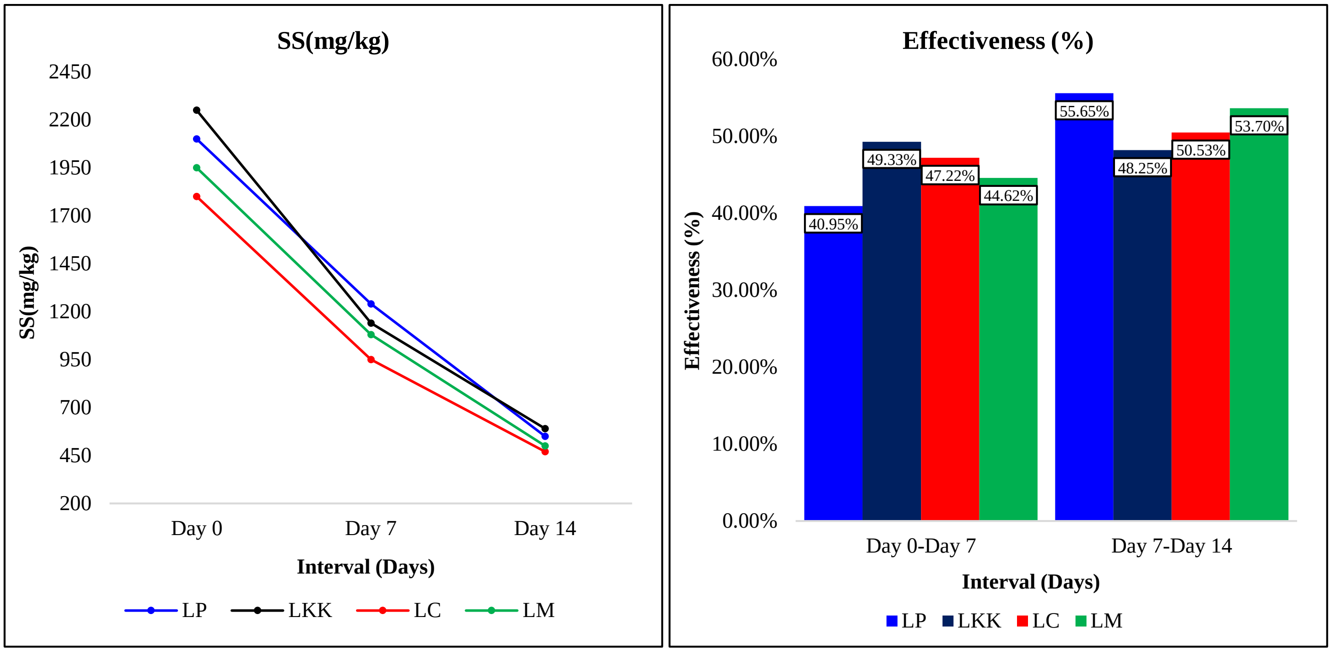

Fig. 25 Soluble salts 14-day prototypes

4.3. Control of 30-Day Prototypes

4.3.1. Moisture Content of 30-Day Prototypes

Over the 30 days of observation, all materials recorded a consistent decline in moisture content, as shown in Table 15. Over the final five days of the monitoring period and the control on Day 33, all materials achieved similar low values for moisture content (near 2.50%). The King Kong brick began with the highest starting moisture content (13.849%) and decreased to 2.510%, with the greatest drops occurring during the first 13 days. The pandereta brick began at 12.568% and ended at 2.511%, with marked decreases during Days 1 to 13, indicating an accelerated drying phase during the first half of the monitoring period. The solid brick began at 11.848% and ended at 2.481%. This brick had a more compacted structure than the others, which contributed to a steadier and intermediate rate of moisture removal. While the concrete block began with the lowest starting moisture content (7.556%), it retained the most moisture with 8.919 V and decreased to 2.468%. This indicates that more electrical energy was consumed to achieve moisture removal similar to that of the ceramic bricks.

Table 15. 30-day prototype humidity monitoring

Type of Brick	Monitoring of prototypes for 30 days + 1 check-up / Every 3 days													
	Theoretical voltage (V)	Humidity (%)												
		Dia 0	Day 1	Day 4	Day 7	Day 10	Day 13	Day 16	Day 19	Day 22	Day 25	Day 28	Day 30	Day 33
LP	1.733	12.568	9.744	7.623	6.112	4.911	4.123	3.551	3.134	2.862	2.681	2.58	2.519	2.511
LKK	1.773	13.849	11.129	8.769	7.024	5.813	4.921	4.265	3.714	3.292	2.951	2.713	2.531	2.51
LC	8.919	7.556	6.271	5.333	4.641	4.133	3.723	3.391	3.123	2.911	2.734	2.593	2.471	2.468
LM	1.126	11.848	9.211	7.363	6.041	5.074	4.362	3.828	3.399	3.071	2.829	2.652	2.498	2.481

Figure 26 shows that all moisture curves followed a continuous downward trend, with steeper slopes in the first 13 days and gradual stabilisation as they approached the target value. The trajectory of both the King Kong brick and pandereta is comparable, showing an early steep decline, followed by Day 28, where they converged towards the reference threshold. The trajectory of the solid brick is also comparable, but shows a slightly less steep curve while maintaining a steady rate of reduction. The concrete block shows the least steep curve from the beginning, and while it shows gentle declines, it demonstrates a slower, but sustained process. One pertinent observation is that, by Day 33, all materials had more or less the same level of moisture. This shows that electro-osmosis is effective in unifying the final results despite the differing composition and porosity.

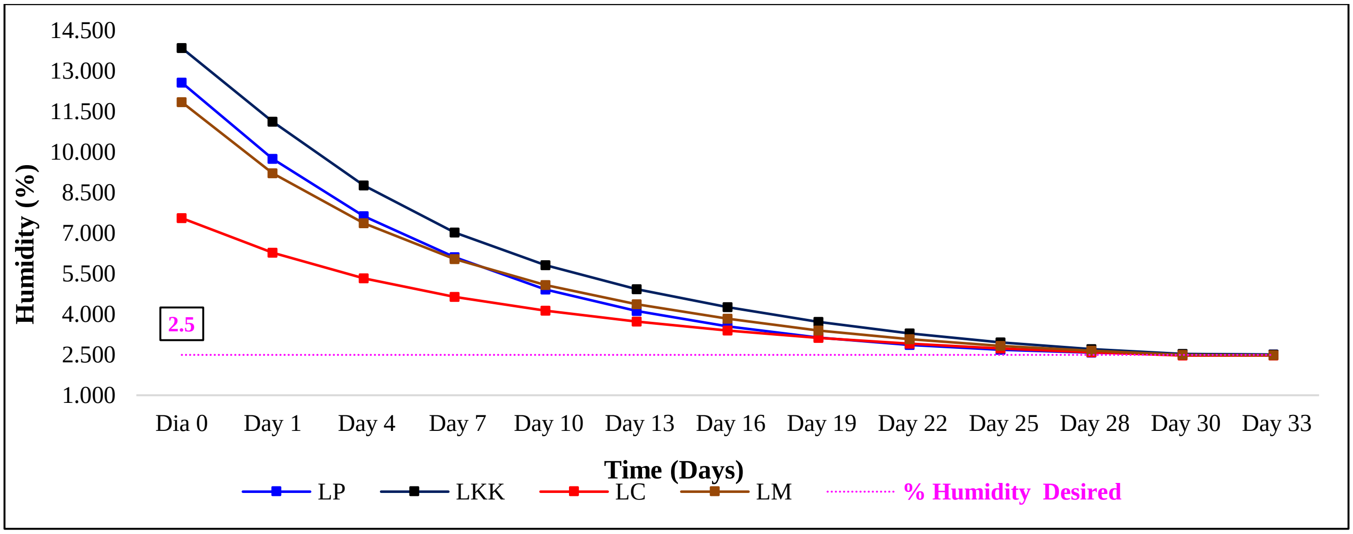

Fig. 26 Humidity monitoring - 30 Days prototypes

In Table 16, we observe that during the 33 days of monitoring, the effectiveness of electro-osmosis decreased progressively in all materials, though the behaviours during the initial phases were different. The pandereta brick, for instance, started at 22.47% and decreased gradually to 0.32%, indicating a significant loss of effectiveness from Day 13 onwards. King Kong brick started at 19.64% and reached 0.83% at the end, notable for its irregular behaviour in the early intervals, where it reached a slight upturn of 21.21% on Day 4 before entering a downward trend. The solid brick started at 22.26%, with regular declines to 0.68%, confirming a sustained and stable reduction. In contrast, concrete blocks showed the lowest values throughout the period, starting at 17.01% and ending at 0.12%, reflecting their lower relative response to treatment, although they maintained a uniform decline without fluctuations.

Table 16. Monitoring moisture effectiveness on 30-day prototypes

Brick Type	Efficacy over time (%) for 30-day prototypes											
	Day 0 - Day 1	Day 1 - Day 4	Day 4 - Day 7	Day 7 - Day 10	Day 10 - Day 13	Day 13 - Day 16	Day 16 - Day 19	Day 19 - Day 22	Day 22 - Day 25	Day 25 - Day 28	Day 28 - Day 30	Day 30 - Day 33
LP	22.47%	21.77%	19.82%	19.65%	16.05%	13.87%	11.74%	8.68%	6.32%	3.77%	2.36%	0.32%
LKK	19.64%	21.21%	19.90%	17.24%	15.34%	13.33%	12.92%	11.36%	10.36%	8.07%	6.71%	0.83%
LC	17.01%	14.96%	12.98%	10.95%	9.92%	8.92%	7.90%	6.79%	6.08%	5.16%	4.70%	0.12%
LM	22.26%	20.06%	17.95%	16.01%	14.03%	12.24%	11.21%	9.65%	7.88%	6.26%	5.81%	0.68%

Figure 27 shows that all efficiency curves followed a downward trend towards Day 33, but with different dynamics depending on the material. The pandereta brick showed a continuous and rapid decline, while the King Kong brick showed a rebound in the early days before aligning with the general trend. The solid brick remained on an intermediate trajectory, without significant fluctuations and with more gradual declines. The concrete block, meanwhile, had the lowest curve from the outset and declined at a less steep slope, reflecting its reduced effectiveness compared to the other materials. Overall, the figure showed that, although ceramic bricks (pandereta, King Kong, and solid) were more effective in the early days, all materials converged towards minimum effectiveness values by Day 33, confirming that the greatest impact of the treatment was concentrated in the initial phase.

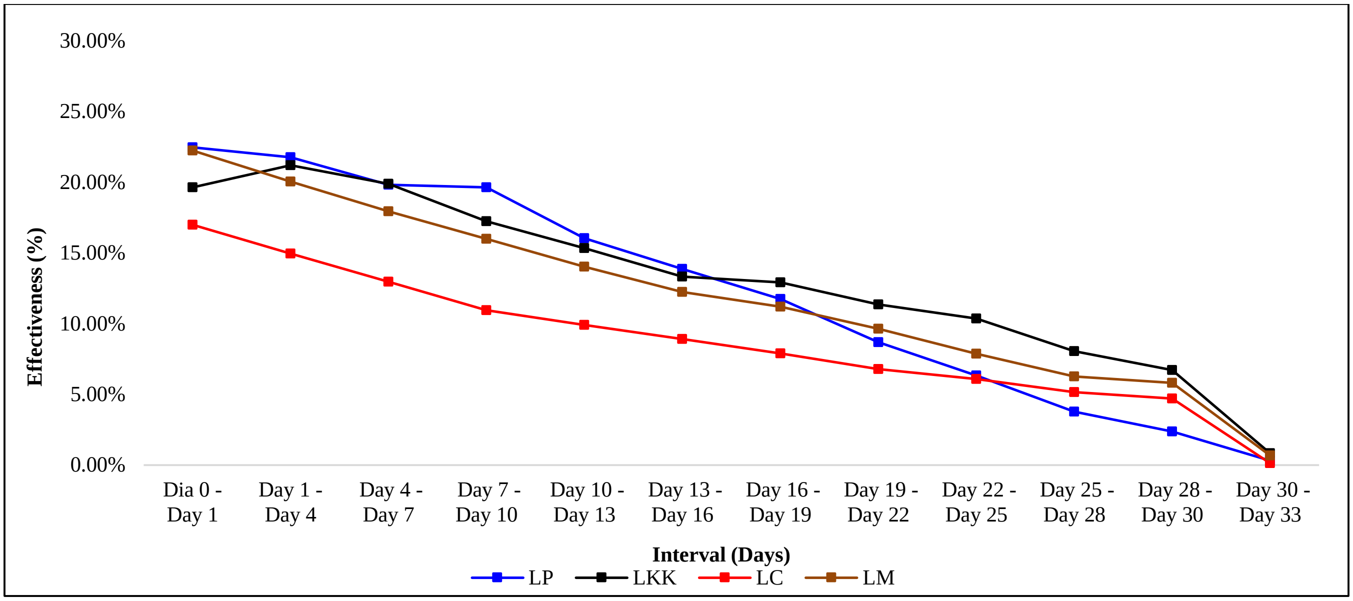

Fig. 27 Humidity effectiveness monitoring - 30 days

4.3.2. Soluble Salts in the 30-Day Prototypes

Table 17 shows significant reductions in salt concentration after 30 days of electro-osmosis application, although with different behaviours depending on the material. The pandereta brick walls (LP) went from 2050 mg/kg to 550 mg/kg, reaching the very low category, which was explained by their high porosity and ease of ion conduction, which allowed for sustained transport throughout the period. King Kong Brick Walls (LKK) decreased from 2300 mg/kg to 850 mg/kg, placing them in the moderate category. This result reflected that, although capillary connectivity favoured initial extraction, a remnant of salts trapped in more internal pores persisted. In the case of Concrete Walls (LC), the concentration dropped from 1850 mg/kg to 650 mg/kg, also at a moderate level; their response was due to the fact that, despite their lower porosity, the application of a higher voltage (8.919 V) allowed salts to be mobilised through microcracks and voids in the material. Finally, Solid Brick Walls (LM) decreased from 1980 mg/kg to 750 mg/kg, remaining in the moderate category; their compactness partially limited migration, although electro-osmosis managed to remove more than 60% of the initial salts. Overall, the results confirmed that at 30 days, all materials showed a sustained decrease, with the pandereta showing the greatest response and King Kong showing the greatest residual resistance.

Table 17. Monitoring soluble salts in 30-day prototypes

Type of Brick	Monitoring at 30 days						
	Theoretical voltage (V)	SS (mg/kg)				Effectiveness by Time	
		Day 0	Day 15	Day 30	Final Condition	Day 0-Day 15	Day 15-Day 30
LP	1.733	2050	1210	550	Very low	40.98%	54.55%
LKK	1.773	2300	1450	850	Moderate	36.96%	41.38%
LC	8.919	1850	1050	650	Moderate	43.24%	38.10%
LM	1.126	1980	1350	750	Moderate	31.82%	44.44%

Figure 28 shows the cumulative percentage efficacy in the intervals Day 0-Day 15 and Day 15-Day 30. In the first fortnight, efficacy ranged from 31.82% to 43.24%, with concrete blocks (43.24%) and pandereta bricks (40.98%) showing the highest initial performance. In the second fortnight, the pandereta brick showed the greatest efficacy, at 54.55%, and clear dominance over other materials. This shows that it still has high rates of salt migration due to its porosity. Concrete blocks lost relative effectiveness at 38.10%, which suggests that after the first phase of purification, the remaining salts were trapped in recesses of the purification matrix. At King Kong Brick and Solid Brick, the efficiencies were 41.38% and 44.44%, respectively, and they showed progressive declines, which we attributed to the removal of salts still present in the finer capillaries of the matrix. Overall, the electro-osmosis effect did not change over the period, and the pandereta showed a gradual and then pronounced effect, which demonstrated that its effect is determined by the mesh structure and the voltage applied.

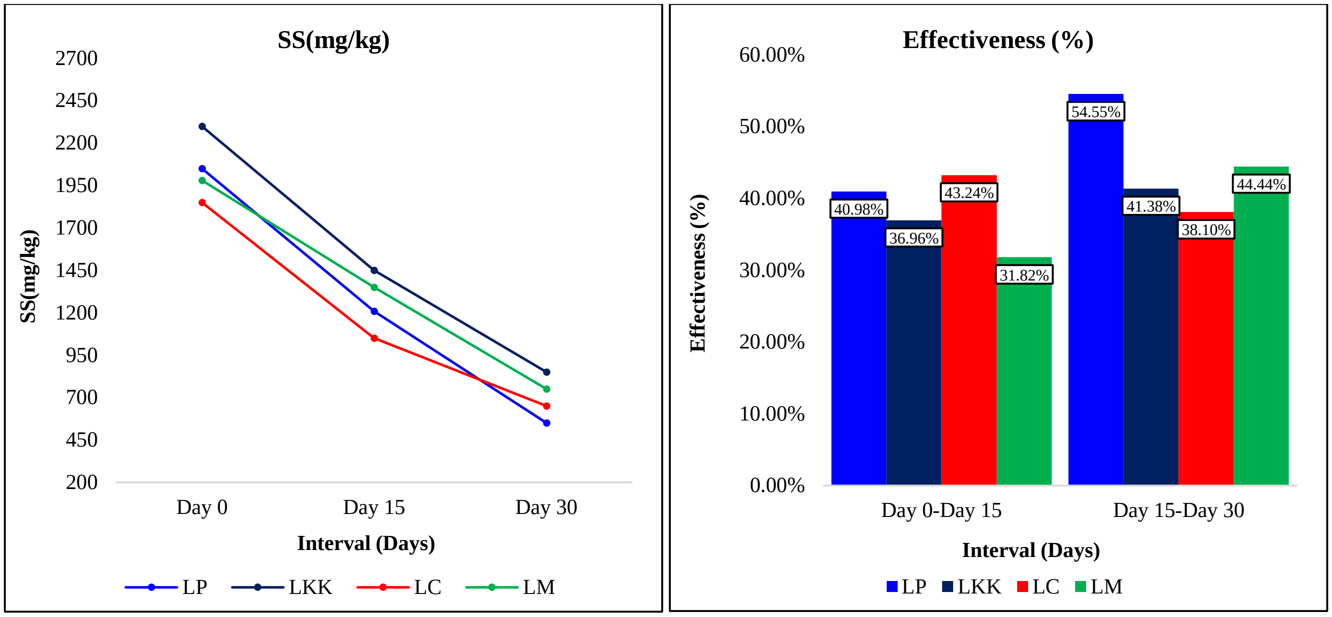

Fig. 28 Soluble salts - 30-day prototypes

4.4. Control of 60-Day Prototypes

4.4.1. Moisture Content of 60-Day Prototypes

Table 18 shows that all materials gradually reduced their moisture content over the 60 days of monitoring, plus an additional control on day 64, reaching final values close to the threshold of 2.50%. The King Kong brick started with the highest moisture content (12.499%) and decreased to 2.461%, with a steady reduction throughout the period. The pandereta brick started at 11.538% and reached 2.495%, notable for a rapid decline in the first 25 days, followed by a gradual stabilisation towards the end. The solid brick started at 10.647% and reached 2.481%, confirming an intermediate and stable behaviour with regular moisture losses in each interval. In contrast, the concrete block, although it started with the lowest value (6.619%), required a higher voltage (3.633 V) and dropped to 2.443%, which showed that its denser cement matrix required more electrical energy to achieve drying equivalent to that of ceramic bricks.

Table 18. Moisture monitoring of 60-day prototypes

Type of Brick	Monitoring of prototypes for 60 days + 1 check-up / Every 4 days																	
	T. Volt. (V)	Humidity (%)																
		Day 0	Day 1	Day 5	Day 9	Day 13	Day 17	Day 21	Day 25	Day 29	Day 33	Day 37	Day 41	Day 45	Day 49	Day 53	Day 57	Dia 60	Day 64
LP	0.778	11.54	9.67	7.91	6.51	5.41	4.50	3.89	3.42	3.09	2.87	2.73	2.64	2.57	2.54	2.52	2.50	2.50	2.50
LKK	0.781	12.50	10.54	8.75	7.24	5.88	4.84	4.12	3.64	3.34	3.11	2.93	2.81	2.70	2.62	2.55	2.50	2.47	2.46
LC	3.633	6.62	5.82	5.13	4.58	4.22	3.94	3.67	3.49	3.32	3.18	3.04	2.91	2.80	2.71	2.62	2.55	2.49	2.44
LM	0.491	10.65	8.70	6.97	5.64	4.83	4.21	3.77	3.43	3.15	2.95	2.81	2.71	2.62	2.56	2.53	2.50	2.50	2.48

As shown in Figure 29, all curves are on a downward continuous line, with the first 20 days of any curve having a tighter slope, while subsequent days are more sloped but still heading to their target value. Results- Time course of change in King Kong brick and pandereta were comparable, with rapid declines starting within the first days and convergence towards the reference line after Day 50. The brick had a lower curve from the start, but with a constant slope that managed to achieve the same final level. Concrete block exhibited the least degree of deflection across the period, with a slow but continuous reduction before it reached similar results to the other materials. In general, therefore, this figure proved that all types of brick, after as much variation with moisture and applied voltage at the beginning, ultimately homongenised each other around 2.5% at the end of the test period, confirming that electro-osmosis does work over longer time frames.

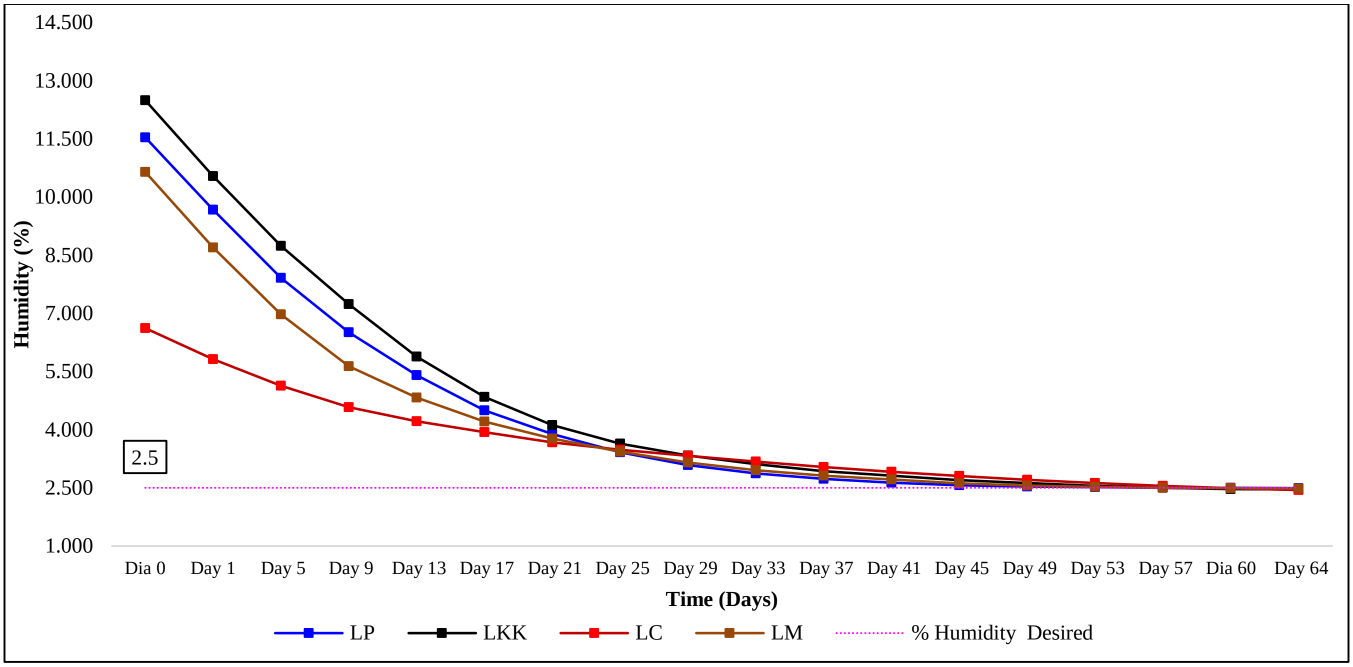

Fig. 29 Humidity monitoring - 60 days prototypes

The efficacy of electro-osmosis declined over the course of 60 days of monitoring, plus Day 64, which served as a control (Table 19), in the four materials. Starting at 16.16% the pandereta brick, after a quick correction higher to 18.19% in five initial days, dropped to 0.12%, an evidence of high early effectivity which diluted by the final section The King Kong brick started the period at 15.67%, peaked on Day 13 at 18.77% and after a very slight downward trend fell to 0.44%, confirming funny business initially but then behaving just like all other bricks towards the end of the observation period. The gradual decline exhibited by solid brick commenced at 18.32%, reached a maximum of 19.83% on day five, and concluded at 0.64%, demonstrating a constant behaviour following its first response during the testing period (Table 3). On the other hand, the concrete block had the lowest values (from 12.13 to 1.93%), followed by a smoother but continuous decline trend, demonstrating that its sensitivity to treatment was lower compared to ceramic bricks.

Table 19. Monitoring of moisture effectiveness in 60-day prototypes

Brick Type	Efficacy over time (%) for 60-day prototypes															
	Day 0 - Day 1	Day 1 - Day 5	Day 5 - Day 9	Day 9 - Day 13	Day 13 - Day 17	Day 17 - Day 21	Day 21 - Day 25	Day 25 - Day 29	Day 29 - Day 33	Day 33 - Day 37	Day 37 - Day 41	Day 41 - Day 45	Day 45 - Day 49	Day 49 - Day 53	Day 53 - Day 57	Day 57 - Dia 60	Day 60 - Day 64
LP	16.16	18.19	17.72	16.91	16.89	13.48	12.21	9.51	7.02	4.94	3.48	2.50	1.36	0.83	0.44	0.24	0.12
LKK	15.67	17.04	17.20	18.77	17.68	14.85	11.64	8.34	6.80	5.78	4.13	3.84	2.96	2.74	1.96	1.16	0.44
LC	12.13	11.76	10.74	7.86	6.75	6.71	5.07	4.65	4.45	4.41	4.12	3.68	3.39	3.17	2.86	2.24	1.93
LM	18.32	19.83	19.12	14.40	12.76	10.40	8.98	8.24	6.32	4.71	3.59	3.36	2.21	1.37	0.99	0.24	0.64

Figure 30 shows that all efficiency curves followed a general downward trend, although with differences in the shape of each trajectory. King Kong brick and solid brick stood out for reaching the highest efficiency peaks in the first fortnight, before aligning with the downward trend of the other materials. The pandereta showed similar behaviour, with a moderate initial rise followed by a continuous decline. The concrete block, on the other hand, remained below the others throughout the test, with a flatter curve reflecting its lower relative effectiveness. By Day 60, all materials converged towards values close to zero, confirming that the most significant impact of electro-osmosis was concentrated in the first 20 days of application, while in subsequent intervals, its effectiveness decreased uniformly across all brick types.

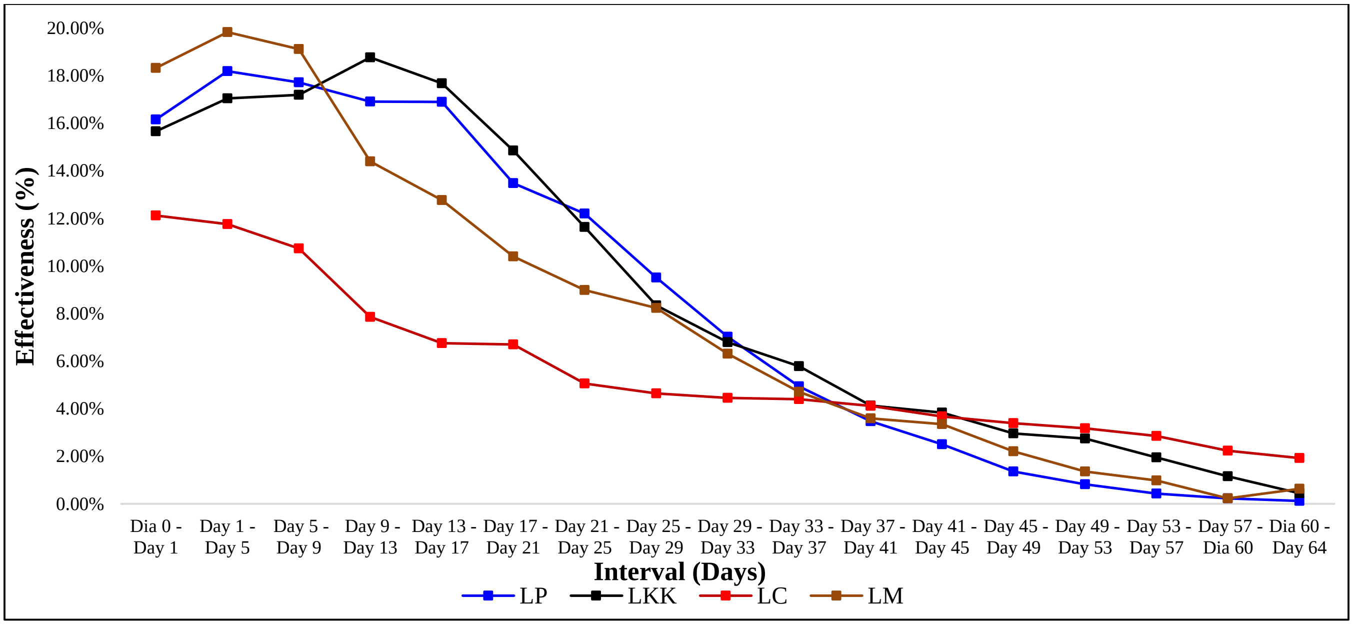

Fig. 30 Salt monitoring, Humidity effectiveness monitoring 60-day prototypes

4.4.2. Soluble Salts at 60 Days

Table 20 shows the notable reductions in salt concentration after 60 days of electro-osmosis application. The pandereta Brick Walls (LP) decreased from 2150 mg/kg to 750 mg/kg, reaching the moderate category; this behaviour was due to the persistence of salts in finer pores, although the high porosity of the material allowed a constant rate of evacuation to be maintained. King Kong Brick Walls (LKK) decreased from 2200 mg/kg to 860 mg/kg, demonstrating a moderate level; the result showed that although their capillary system enabled initial extraction, significant salt still remained in inaccessible areas even after two months. In concrete walls (LC), the reduction was from 1600 mg/kg to 650 mg/kg, remaining in moderate condition; this behaviour was associated with the need to apply a higher Voltage (3.633 V) to compensate for the low porosity of its matrix, achieving effective but slower migration. Finally, Solid Brick Walls (LM) decreased from 1850 mg/kg to 590 mg/kg, reaching the very low category; their response was explained by the prolonged action of the electric field, which allowed the salts to be progressively extracted from their accessible pores, despite their initial compactness. Overall, the results confirmed that, at 60 days, electro-osmosis maintained its effectiveness, achieving more marked reductions in compact materials such as solid brick and stabilising the values in the other materials.

Table 20. Monitoring of soluble salts in 60-day prototypes

Type of Brick	Monitoring of 60-day prototypes						
	Theoretical voltage (V)	SS (mg/kg)				Effectiveness over time	
		Day 0	Day 30	Day 60	Final Condition	Day 0-Day 30	Day 30-Day 60
LP	0.778	2150	1280	750	Moderate	40.47%	41.41%
LKK	0.781	2200	1370	860	Moderate	37.73%	37.23%
LC	3.633	1600	1110	650	Moderate	30.63%	41.44%
LM	0.491	1850	1210	590	Very low	34.59%	51.24%

Figure 31 shows the effectiveness of salt reduction by intervals. Between Day 0 and Day 30, the efficiencies ranged from 30.63% to 40.47%, with the pandereta brick (40.47%) and the King Kong brick (37.73%) showing the best initial results. In the second phase, from Day 30 to Day 60, the efficiencies increased in most materials, with the solid brick (51.24%) standing out as the best performer, followed by the concrete block (41.44%). This behaviour indicated that, while in the first 30 days mainly the most soluble salts were removed, in the second interval the electric current managed to mobilise salts retained in micro-pores and denser areas, increasing the cumulative efficacy. Overall, the graph showed that electro-osmosis maintained an active and sustained process, with a tendency towards stabilisation in materials such as pandereta and King Kong, and a more favourable response in solid brick towards the end of the period.

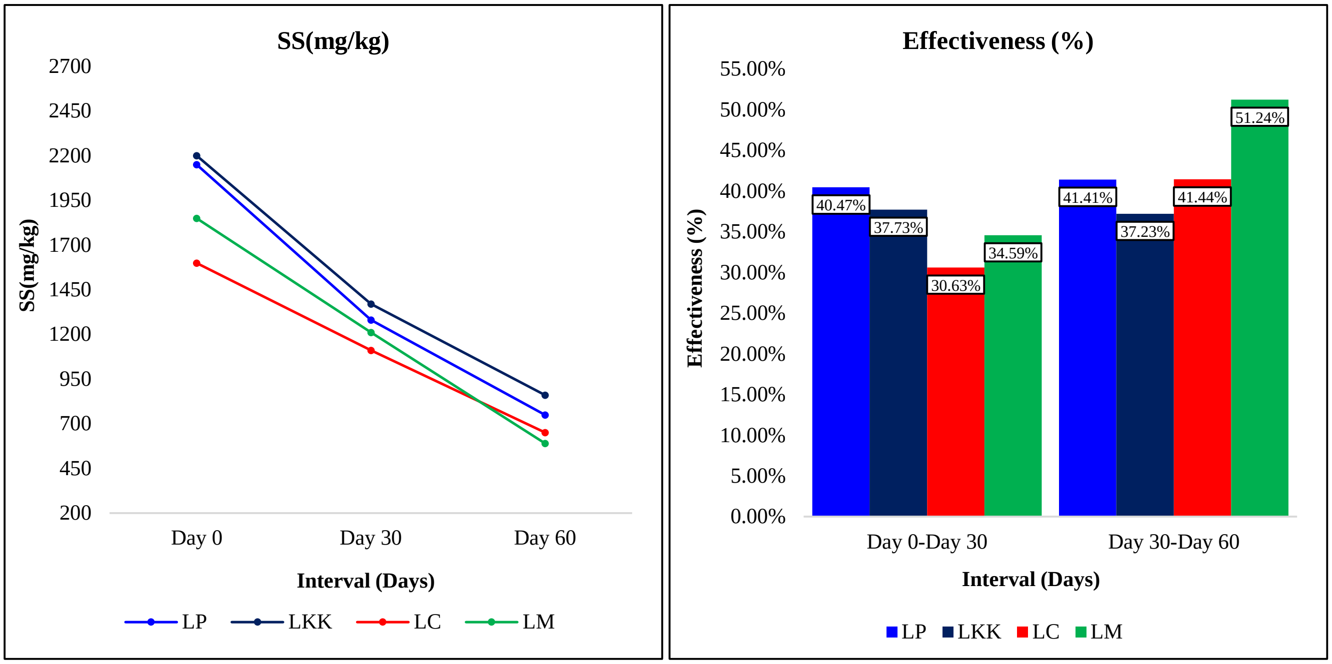

Fig. 31 Soluble salts 60-day prototypes

4.5. Control of 90-Day Prototypes

4.5.1. Moisture Content of 90-Day Prototypes

Table 21 shows that the four materials continuously reduced their moisture content throughout the 90 days of monitoring, plus a control on Day 97, reaching final values very close to the reference threshold of 2.50%. The King Kong brick started with the highest moisture content (13.611%) and decreased to 2.381%, notable for an accelerated reduction in the first 29 days, followed by a more gradual decrease. The pandereta brick started at 12.851% and reached 2.398%, showing a similar pattern with sharp drops in the first weeks and stabilisation towards the end. The solid brick started at 11.616% and fell to 2.482%, confirming an intermediate and sustained behaviour throughout the period. Concrete blocks had the lowest initial value (7.418%) and ended at 2.461%, requiring a higher voltage (2.892 V) to achieve the same drying condition, which demonstrated the greater resistance of their cement matrix to electro-osmotic flow.

Table 21. Moisture monitoring of 90-day prototypes

Brick Type	Monitoring of Prototypes for 90 Days + 1 check-up / Every 7 Days															
	T. Volt. (V)	Humidity (%)														
		Dia 0	Day 1	Day 8	Day 15	Day 22	Day 29	Day 36	Day 43	Day 50	Day 57	Day 64	Day 71	Day 78	Day 85	Day 90	Day 97
LP	0.594	12.851	10.521	8.461	6.728	5.381	4.385	3.751	3.341	3.101	2.943	2.802	2.678	2.566	2.485	2.415	2.398
LKK	0.579	13.611	11.069	9.262	7.786	6.617	5.692	4.953	4.354	3.886	3.491	3.174	2.923	2.721	2.544	2.431	2.381
LC	2.892	7.418	5.987	5.109	4.379	3.789	3.498	3.281	3.096	2.924	2.816	2.713	2.619	2.551	2.513	2.483	2.461
LM	0.366	11.616	9.561	7.564	6.129	5.091	4.354	3.831	3.459	3.174	2.966	2.818	2.688	2.602	2.541	2.496	2.482

Figure 32 shows that the curves for all materials followed a well-defined downward trend, with steeper slopes in the first 30 days and a gradual flattening as they approached the target level. King Kong brick remained the highest curve for much of the test, followed closely by pandereta, both with initial steep reductions. The solid brick showed an intermediate curve, with a stable and continuous rate of decline, while the concrete block had the lowest curve from the start, but with a gentler slope that showed a slower, yet equally effective, process. By Day 90, all curves converged around the reference value, confirming that electro-osmosis allowed for the homogenisation of moisture in different materials, even under prolonged monitoring conditions.

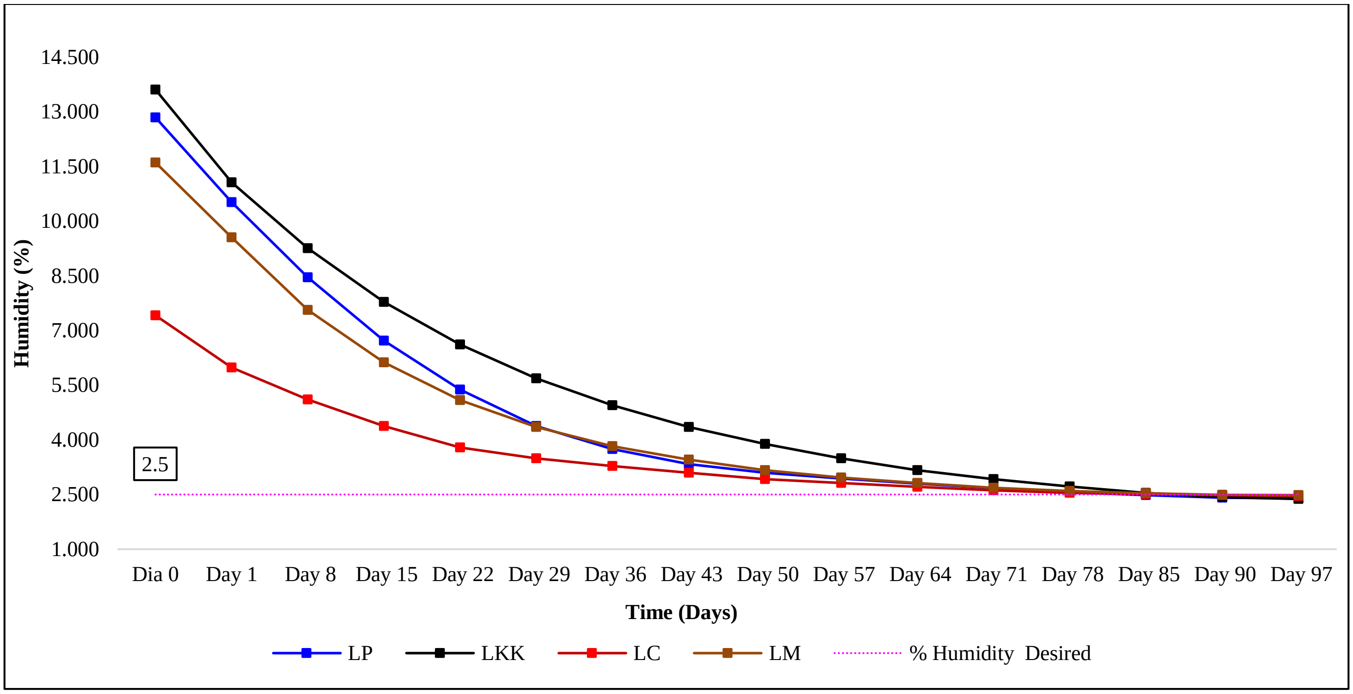

Fig. 32 Humidity monitoring - 90 Days prototypes

Table 22 shows that the effectiveness of electro-osmosis in the four materials decreased over the 90 days of monitoring, plus the control on Day 97, although with nuances in each type of brick. The pandereta brick started at 18.13% and reached a maximum of 20.48% on Day 15, then declined steadily to 0.70% at the end, reflecting high initial effectiveness followed by progressive loss. The King Kong brick started at 18.68% and maintained effectiveness between 15% and 13% until Day 29, before gradually declining to 2.06%, confirming a more stable performance in the first half of the trial. The solid brick started at 17.69% and recorded a one-off increase to 20.89% on Day 8, before beginning a steady decline to 0.56%, showing a favourable response in the initial phase. Compared to the others, the concrete block, despite starting at 19.29%, was the one to lose effectiveness the fastest, from 19.29% to 7.68% by Day 29 and finishing at 0.89%, showing it was less effective than ceramic materials.

Table 22. Monitoring moisture effectiveness in 90-day prototypes

Brick Type	Efficacy by time (%) at 90 days														
	Day 0 - Day 1	Day 1 - Day 8	Day 8 - Day 15	Day 15 - Day 22	Day 22 - Day 29	Day 29 - Day 36	Day 36 - Day 43	Day 43 - Day 50	Day 50 - Day 57	Day 57 - Day 64	Day 64 - Day 71	Day 71 - Day 78	Day 78 - Day 85	Day 85 - Day 90	Day 90 - Day 97
LP	18.13	19.58	20.48	20.02	18.51	14.46	10.93	7.18	5.10	4.79	4.43	4.18	3.16	2.82	0.70
LKK	18.68	16.32	15.94	15.01	13.98	12.98	12.09	10.75	10.16	9.08	7.91	6.91	6.50	4.44	2.06
LC	19.29	14.67	14.29	13.47	7.68	6.20	5.64	5.56	3.69	3.66	3.46	2.60	1.49	1.19	0.89
LM	17.69	20.89	18.97	16.94	14.48	12.01	9.71	8.24	6.55	4.99	4.61	3.20	2.34	1.77	0.56

While every efficiency curve exhibited an overall downward tendency, Figure 33 shows deficiencies in every efficiency curve. The pandereta brick was one of the most effective for the first 20 days, before its decline. The "King Kong" brick was not an exception to the general decline; however, it exhibited stronger stability over time, as it was accompanied by more gradual deviations, exhibiting more consistent dissipation of efficacy. The solid brick was distinctive in that it exhibited an initial peak in efficacy before aligning with the general dissipation of the other bricks. The concrete brick was exceptionally dull in that its dissipation was most consistent, as it exhibited the lowest efficiency curve from the first 5 days of the testing, showing its lowest sensitivity to the process. All bricks exhibiting the general dissipation of efficacy finally converged at a value below 3% by day 90, showing in unison the most evident suppression of electro-osmosis in the post-initial treatment.

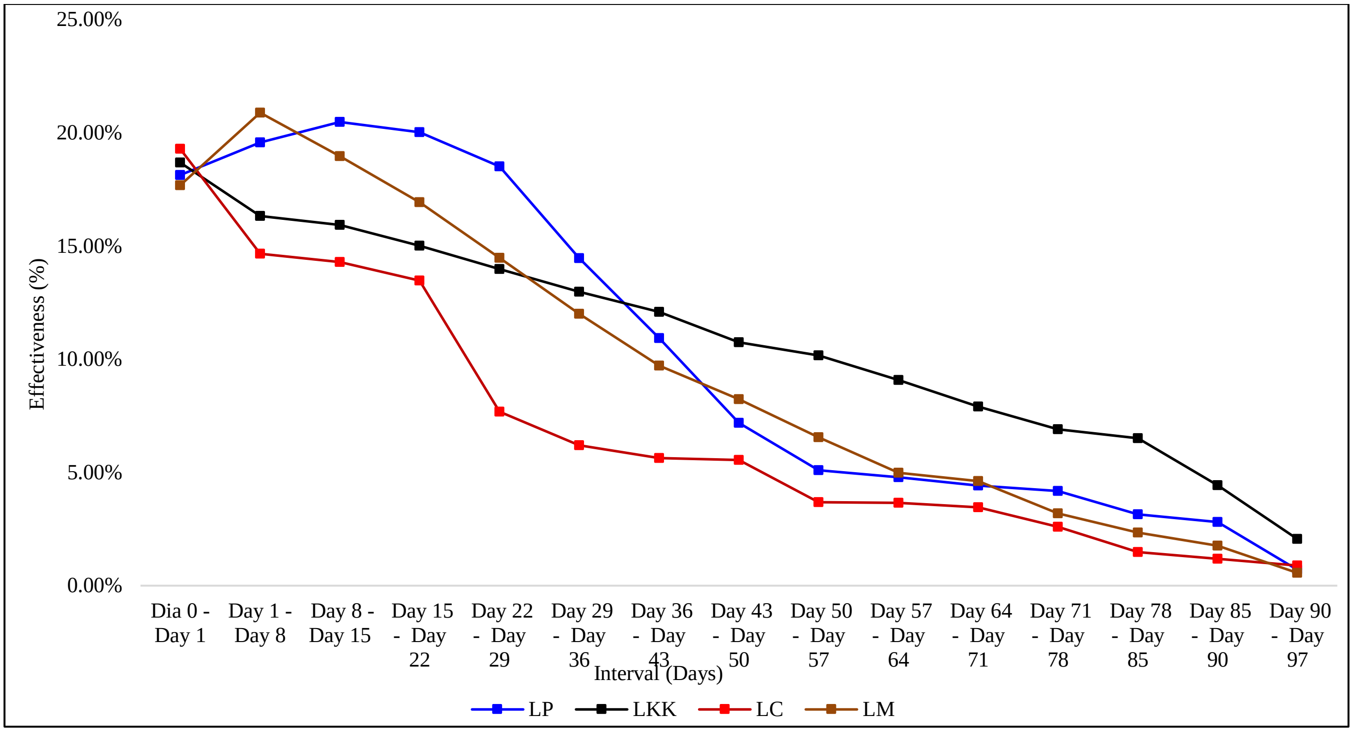

Fig. 33 Salt monitoring, humidity effectiveness monitoring 90-day prototypes

4.5.2. Soluble Salts at 90 Days

Table 23 shows that, after 90 days of electro-osmosis application, all wall prototypes achieved a significant reduction in their initial salt concentrations, although without reaching very low category values. The pandereta Brick Walls (LP) went from 2000 mg/kg to 690 mg/kg, placing them in moderate condition; this decrease was explained by their high porosity, which favoured sustained ionic conduction throughout the test. King Kong Brick Walls (LKK) decreased from 2150 mg/kg to 850 mg/kg, remaining in moderate condition; their higher initial accumulation and the presence of salts trapped in internal capillaries prevented them from reaching lower levels. In the case of concrete walls (LC), the values decreased from 1700 mg/kg to 640 mg/kg, which represented one of the most significant reductions despite their low porosity. This result was possible thanks to the application of a higher voltage (2.892 V), which allowed salts to be mobilised through microcracks and the hydration network of the cementitious matrix. Finally, Solid Brick Walls (LM) showed reductions from 1800 mg/kg to 790 mg/kg, also reaching moderate condition; the compactness of the material obstructed ion migration, which explained the lower relative performance compared to pandereta and concrete. The results confirmed that, even though all materials at Day 90 still remained with moderate levels of residual salts, the sustained reductions were indicative of the continued effectiveness of electro-osmosis.

Table 23. Monitoring soluble salts in 90-day prototypes

Type of Brick	Monitoring of 90-Day Prototypes						
	Theoretical voltage (V)	SS (mg/kg)				Effectiveness over time	
		Day 0	Day 45	Day 90	Final Condition	Day 0-Day 45	Day 45-Day 90
LP	0.594	2000	1250	690	Moderate	37.50%	44.80%
LKK	0.579	2150	1370	850	Moderate	36.28%	37.96%
LC	2.892	1700	1050	640	Moderate	38.24%	39.05%
LM	0.366	1800	1150	790	Moderate	36.11%	31.30%

Figure 34 illustrates the efficacy percentage obtained during the 0-45 and 45-90 day intervals. In the first phase, efficacy ranged from 36% to 38%, with concrete blocks (38.24%) and pandereta bricks (37.50%) showing the highest initial response. In the second phase, the pandereta brick again showed the best performance (44.80%), reflecting the advantage of its high porosity in maintaining continuous salt transport. Concrete blocks (39.05%) and King Kong bricks

(37.96%) maintained intermediate efficiencies, showing that, although the process continued to be effective, the rate of extraction slowed as the most soluble fractions were depleted. In contrast, the solid brick (31.30%) showed the lowest efficiency in the second section, confirming that the density and low connectivity of its pores limited the prolonged action of electro-osmosis. Overall, the graph showed a stabilisation trend towards the end of the test, where most of the easily migratable salts had already been removed, leaving mainly less accessible residual salts.

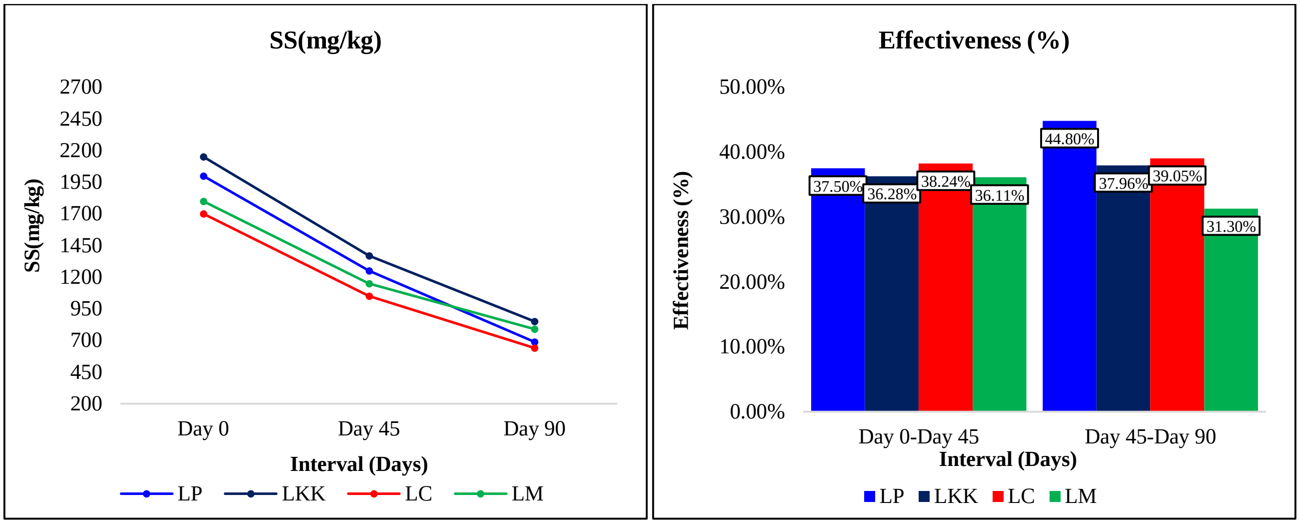

Fig. 34 Soluble salts - 90-day prototypes

4.6. Optimal Configuration

According to the results obtained, the optimal operating time was 14 days, since at this time frame all wall prototypes simultaneously reached the reference humidity of 2.50% and a very low salt concentration (≤ 600 mg/kg), as shown in Table 24. At 7 days, moderate salt values still persisted, while at 30, 60, and 90 days, although additional decreases were observed, the reductions were less significant compared to the increase in time and energy consumed. Therefore, it was determined that the best working condition corresponds to 14 days with the specific voltages calculated for each material, which allowed the initial moisture content to be reduced to below the established target of 2.50% and to decrease the initial salts (1700-2250 mg/kg) to final values between 470 and 590 mg/kg, ensuring a stable condition with a low risk of efflorescence.

Table 24. Optimal configuration conditions

Material	Theoretical voltage (V)	Initial moisture content (%)	Actual final moisture content (%)	Initial salts (mg/kg)	Final salts (mg/kg)	Final condition
LP	**3.637**	12.359	2.491	2100	550	Very low
LKK	**3.419**	12.712	2.479	2250	590	Very low
LC	**16.296**	6.811	2.481	1800	470	Very low
LM	**2.183**	10.957	2.468	1950	500	Very low

4.7. Sustainability and Economic Analysis

Table 25 shows the cost of implementing the electro-osmotic system based on operating time and volume of water removed. These calculations were based on the electrical resistivity values determined for each type of brick according to its moisture content [65, 66]. With the voltage applied, the Equivalent Resistance (R) was obtained and, from this, the current (I). Subsequently, using the expression $E=V\cdot I\cdot t$ [67], the Energy Consumed (kWh) was calculated and, finally, the total cost per 1m2 of treated wall. In the 7-day tests, the costs were high due to the high initial voltages required to induce electro-osmotic migration in walls that were still saturated: concrete (S/ 6,848), King Kong (S/ 3,839), pandereta (S/ 2,111), and solid (S/ 0.530). By extending the operation to 14 days, which was considered the optimal technical and economic condition, costs were significantly reduced because the working voltages decreased as the resistivity of the material increased with moisture loss. At this point, high salt removal efficiency (category 'very low') was achieved simultaneously with much more affordable unit costs: pandereta (S/ 1,066), King Kong (S/ 1,153), concrete (S/ 1,904), and solid (S/ 0.131). At 30 days, although salt removal continued, the marginal benefit was reduced compared to the increase in application time, as most of the soluble salts had been removed in the first 14 days. The cumulative costs were S/ 0.585 (pandereta), S/ 1.551 (King Kong), S/ 2.047 (concrete), and S/ 0.165 (solid), which showed that the additional expenditure did not translate into proportional improvements in effectiveness. Over longer periods (60 and 90 days), the required voltages dropped to very low levels due to the progressive reduction of water available in the pores, which decreased energy consumption and allowed for even lower unit costs (S/ 0.130 to 0.364 at 60 days and S/ 0.046-0.584 at 90 days). However, in these intervals, the effectiveness of the process had already stabilised, so extending the application did not represent a significant advantage in terms of energy consumption or time invested. In summary, the analysis of costs per m² of wall confirms that 14 days offers the best cost-benefit ratio, achieving critical reductions in salt content and sustained decreases in humidity with reasonable energy expenditure. Based on these unit values, costs can be scaled proportionally to actual wall dimensions by multiplying by the treated area and adjusting according to the number of electrodes and the electrical configuration used.

Table 25. Cost of applying electro-osmosis per 1m2

Time of Use	Volts (V)	Electrical Resistivity of the Material (Ω·m)	R	Current (A)	Time (h)	Energy Consumed (kWh)	Cost per (kWh)	Total Cost (S/.)
Pandereta Brick								
For 7 Days	7.264	25.9	2590	0.00280	168	3.423	0.617	2.111
For 14 Days	3.637	25.7	2570	0.00142	336	1.730	0.617	1.066
For 30 Days	1.733	22.8	2280	0.00076	720	0.949	0.617	0.585
For 60 Days	0.778	41.3	4130	0.00019	1440	0.211	0.617	0.130
For 90 Days	0.594	19.4	1940	0.00031	2160	0.393	0.617	0.242
King Kong brick with 18 holes								
For 7 Days	7.203	14.0	1400	0.00515	168	6.226	0.617	3.839
For 14 Days	3.419	21.0	2100	0.00163	336	1.870	0.617	1.153
For 30 Days	1.773	9.0	900	0.00197	720	2.515	0.617	1.551
For 60 Days	0.781	24.1	2410	0.00032	1440	0.365	0.617	0.225
For 90 Days	0.579	11.2	1120	0.00052	2160	0.646	0.617	0.398
Concrete block								
For 7 Days	36.472	201.2	20120	0.00181	168	11.107	0.617	6.848
For 14 Days	16.296	288.9	28890	0.00056	336	3.089	0.617	1.904
For 30 Days	8.919	172.5	17250	0.00052	720	3.320	0.617	2.047
For 60 Days	3.633	322.1	32210	0.00011	1440	0.590	0.617	0.364
For 90 Days	2.892	190.6	19060	0.00015	2160	0.948	0.617	0.584
Solid brick								
For 7 Days	4.645	42.2	4220	0.00110	168	0.859	0.617	0.530
For 14 Days	2.183	75.6	7560	0.00029	336	0.212	0.617	0.131
For 30 Days	1.126	34.2	3420	0.00033	720	0.267	0.617	0.165
For 60 Days	0.491	104.5	10450	0.00005	1440	0.033	0.617	0.020
For 90 Days	0.366	38.5	3850	0.00010	2160	0.075	0.617	0.046

From a sustainability perspective, electro-osmosis offers several advantages over conventional moisture control methods. The system operates without chemical additives and is minimally invasive, thereby preserving the integrity of the structure. In addition, energy consumption decreases progressively as the walls dry, which reduces operational demand over time.

The optimal condition identified at 14 days represents the most favourable balance between treatment efficiency and energy consumption, achieving significant reductions in both moisture and soluble salts with moderate electrical input. This behaviour supports the classification of electro-osmosis as an energy-efficient and environmentally favourable technique for application in coastal masonry structures.

5. Recommendations

Electro-osmosis is very effective under environmental conditions and well-suited to high salinity/humidity regions. In this study, which has been conducted in a relevant environment (Peruvian coastal) to the complete methodology and technique published worldwide, so much so that very efficient results have been obtained regarding moisture and soluble salts reduction in masonry materials. This behaviour corresponds to a state of sustained moisture in the pore structure, which promotes electrokinetic transport. On the other hand, increased water within the pores, given lower relative humidity or drier climatic conditions, may not be enough to ensure that electro-osmotic flow takes place with a satisfactory efficiency. This means that electro-osmosis is best suited in coastal and humid environments, areas of high occurrence and long-term rising damp, and where traditional methods have often limited performance.

Long-term performance of electro-osmosis is closely related to the moisture retention and salt removal capacity over time and follows a progressive behaviour recorded in three operational periods of 7 to 90 days. It is concluded that the process stabilizes with long-term operation, showing that it is possible to achieve permanent improvements of masonry elements. However, the persistence of the technique is inherently related to its constant application since electro-osmosis needs a permanent electric field to keep water transferring through the pore matrix. This means that the system needs to ensure continuity and functional integrity of the components over time. Regular monitoring of the system and routine maintenance of electrical components (e.g., electrodes, power supply units) is thus essential for sustained long-term performance.

In conclusion, the validation of electro-osmosis under real-scale conditions and in actual climatic regions and construction typologies, especially the large variety of existing buildings subject to differing environmental and operational factors, should be high on the industry agenda for future research. The system needs to be assessed over the long term, also for the stability of the system, and to check its performance concerning changing environmental conditions. It is also necessary to establish standardised technical criteria for system design and implementation, including voltage selection, electrode configuration, and monitoring procedures based on the electrokinetic properties of masonry materials. In the Peruvian context, the development of technical guidelines would support the consistent and safe application of this technique in construction practice.

6. Discussion

According to research conducted on the application of an electro-osmosis system in the historic Gül Mosque in Istanbul, the moisture content in the walls decreased from an initial level of 14.48% to 2.90%, reaching a ‘dry’ state in approximately nine months of continuous operation. During the first 134 days, 66,550 kg of water (more than 60% of the total) was expelled, while in the following periods the reduction was progressively lower, until it stabilised [21]. In this study, Peruvian masonry walls (pandereta, King Kong, solid, and concrete) started with initial moisture levels between 6.6% and 13.8%, depending on the material, and managed to drop to the optimal reference value of 2.50% in much shorter periods of time. For example, pandereta brick reduced its moisture content from 12.359% to 2.491% in 14 days, while King Kong brick went from 12.712% to 2.479% in the same period. Solid bricks decreased from 10.957% to 2.468% and concrete blocks from 6.811% to 2.481%, all reaching optimal conditions with different voltages (between 2.18 V and 16.29 V). At the same time, the initial soluble salts, which varied between 1800 and 2250 mg/kg, fell to values between 470 and 590 mg/kg, classified as ‘very low’ in terms of efflorescence risk. The differences between the two studies are due to the nature of the materials and environmental conditions. In the Gül Mosque, the thick stone and brick walls, in permanent contact with the marine water table, required prolonged periods to reach stabilisation. In contrast, in the Peruvian masonry walls (pandereta, King Kong, solid and concrete), which were thinner and had greater capillarity, the migration of moisture and salts occurred more rapidly, allowing optimal stable reduction levels to be reached in 14 days.

According to research carried out on an 18th-century heritage building in Europe, the application of an electro-osmotic system made it possible to progressively reduce moisture in walls affected by rising damp. During the first six months, a notable decrease in damp patches and salt efflorescence was observed, and after one year, the moisture content fell to levels considered safe for the stability of the materials [22]. In this study, Peruvian masonry walls showed a much faster and more controlled reduction thanks to the definition of specific voltages for each material and time horizon. In particular, at 14 days, optimal humidity and a very low salt concentration were simultaneously achieved with differentiated voltages (2.18 V for solid masonry, 3.41 V for King Kong, 3.63 V for pandereta, and 16.29 V for concrete). This condition was identified as the most efficient in technical and economic terms, as it allowed significant reductions to be achieved in a short period of time, avoiding unnecessary increases in energy costs over longer periods. The difference concerns the methodology used in measuring the effectiveness of electro-osmosis, which was mainly evaluative due to the fact that the researchers had to rely on observations of the reduction of damp patches and salt efflorescence on the walls over a period of time of up to one year. This method demonstrated, to a degree, the effectiveness of the treatment in a historic building, but it also measured moisture and salts.

The outcome of electro-osmosis in bricks has been studied before, and the findings indicate that the outcome of the process is dependent on the porous structure and the level of capillary connectivity of the material. In the research conducted on four types of Danish bricks, the ones that are more interconnected and have more fine pores (in particular, the Dalum bricks) had the highest electro-osmotic coefficients, and a chloride desalination efficiency of 58.22%. Conversely, the bricks that had a more lowly situated porosity or heterogeneous pore size distribution demonstrated considerably lower fractions of salt content, demonstrating that the treatment microstructure is a vital parameter as stated in the literature [23]. This study corroborated the "classic" literature mention of the microstructure relationship with salt reduction and, more so, pioneered a "new" class of efficiency with Peruvian masonry walls, which started with the initial concentrations of 1800-2250 mg/kg, and the electro-osmosis process resulted in the final concentrations of 470-590 mg/kg.

This above 70 - 75 % efficiency is attributed to the higher capillarity and porosity of the pandereta and King Kong bricks in comparison to low-permeable materials like solid masonry and concrete. Therefore, similar to the Danish study, porosity and pore connectivity were the determining factors, albeit in the Peruvian context, the technique achieved faster and more effective reductions.

7. Conclusion

First, the study proved that at different time intervals, electro-osmosis remained a positive technique in reducing moisture and salts in masonry walls, even under saline conditions. It was possible to attain and maintain levels below the hygroscopic moisture threshold (2.50%) and decrease to some extent the hygroscopic salts, with variations attributable to the type of material and time of application. The findings, in general, affirmed the method as a conservational technique, replicable, sustainable, and viable for the preservation of structures.

Secondly, after applying electro-osmosis for 7 days, the moisture content of the pandereta brick decreased significantly from 12.34% to 2.47%, a reduction associated with its high porosity and thin configuration, which enhances water migration under an electric field. Concurrently, the soluble salt content decreased from 2050 mg/kg to 800 mg/kg, indicating that its lightweight structure facilitated both rapid moisture removal and sustained electrical conductivity. In the King Kong brick, moisture content decreased from 13.25% to 2.46%, while soluble salts were reduced from 2200 to 750 mg/kg, a behaviour attributed to the presence of perforations, which, although favouring salt accumulation, also enhanced their removal under the applied electric gradient. For the concrete block, moisture was reduced from 7.32% to 2.48% and salts from 1750 to 610 mg/kg, achieved by applying a higher voltage (36.47 V) necessary to overcome the low porosity and dense cementitious matrix. Finally, in the solid brick, the moisture content decreased from 11.49% to 2.46% and the salts from 1850 to 650 mg/kg, demonstrating that even a dense material responds effectively during the initial stage due to the progressive action of electric current through its accessible pore network.

Thirdly, electro-osmosis applied to 14-day prototypes consolidated the most efficient horizon of the process. In the pandereta brick, moisture stabilised at 2.49% and salts decreased to 550 mg/kg, thanks to its high permeability, sustaining continuous migration of water and ions. In the King Kong brick, the values decreased from 12.71% to 2.47% in moisture and from 2250 to 590 mg/kg in salts, which was explained by the capillary connectivity of its perforations, which allowed for sustained emptying in the second week. In the concrete block, moisture reached 2.48% and salts 470 mg/kg, demonstrating that, although its density requires higher voltages, conduction was achieved through microcracks and hydration networks. In the solid brick, moisture dropped to 2.46% and salts to 500 mg/kg, confirming that, despite its compactness, the electric field managed to progressively extract the retained ions. This time horizon was consolidated as the most favourable, as all materials simultaneously reached the ‘very low’ condition in salts.

Fourthly, electro-osmosis configured for 30 days of application resulted in stable moisture maintenance (12.57% to 2.51%) and a reduction in salts to 550 mg/kg in the pandereta brick, remaining at a ‘very low’ level. This result was explained by the ease of conduction of its structure, which had already reached its maximum efficiency in the first two weeks. In the King Kong brick, moisture was reduced from 13.85% to 2.51%, but salts remained at 850 mg/kg (moderate), indicating that some of the ions were trapped in deep areas of the capillaries. In the concrete block, the reduction in moisture to 2.46% and salts to 650 mg/kg reflected that prolonging the time did not substantially improve its response, as the denser spaces limited ion migration. In the solid brick, moisture decreased to 2.48% and salts to 750 mg/kg, remaining in moderate condition; this behaviour showed that, after initial purification, additional extraction became marginal.

Fifth, stable desaturation of all masonry units driven by operational electro-osmosis applied for 60 days has been observed, albeit with limited contribution of increased salt removal rates compared to the case achieved in sodium chloride solutions when operated under similar conditions for only a 14-day duration. So, in the pandereta brick, moisture was reduced from 11.54% to 2.50%, and soluble salts to 750 mg/kg (moderate condition). This behaviour suggests that although the porous structure allowed continuous migration of ions, most of the effective removal took place at the initial stages. The moisture of King Kong brick was reduced by 12.50% to 2.46 %, and Salts reached the value of 860 mg/kg, likewise remaining in the moderate category, which indicates that some fraction of ions remain localized at less accessible capillary zones.] Although the treatment duration reached over 16 months, moisture contents and salts in concrete block reduced from 6.62% to 2.44% and to a value of 650 mg/kg, respectively, confirming that additional reduction was hindered by the denser cementitious matrix formed after initial saturation (shown previously)61510. Consequently, in the dense brick, moisture fell from 10.65% to 2.48% and salts to 590 mg/kg —a very low state— challenges that proved that, with time, the electric field was still capable of continuously solubilising salts from the accessible pore network of this dense material.

Sixthly, electro-osmosis configured for 90 days of application caused a reduction in moisture to 2.39% and salts to 690 mg/kg in the pandereta brick, remaining in moderate condition; this was explained because, after the initial phase, the process only mobilised less accessible residual salts. In the King Kong brick, moisture decreased to 2.38% and salts to 850 mg/kg, confirming that, although drying was complete, the presence of internal capillaries retained some of the salts. In the concrete block, the moisture content dropped to 2.46% and the salts to 640 mg/kg, reflecting that its dense matrix allowed it to maintain favourable performance under adequate voltages. In the solid brick, the moisture content reached 2.48% and the salts 790 mg/kg, remaining in moderate condition; its compactness explained the persistence of a remnant of salts that had not been evacuated.

Finally, the results established that the 14-day horizon was optimal, as it allowed the hygroscopic reference humidity to be reached and reduced salts to 'very low' levels in all materials, at a reasonable energy cost. Extending the treatment to 30, 60, or 90 days did not provide proportional benefits, as the additional improvements were marginal compared to the increase in time and energy. It is therefore recommended to implement electro-osmosis under the 14-day configuration, adjusting the voltages to each type of brick, in order to consolidate a technically and economically viable strategy for the conservation of coastal housing and the reduction of risks associated with salt moisture.

Conflicts of Interest

We declare that there is no conflict of interest regarding the publication of this article.

References

[1] Simon Ayernor Tetteh, Isaac Akwei, and George Andoh, "Rising Damp in Buildings: Causes, Impacts, and Mitigation Strategies in Krofrom and Ampabame New Sites," *Asian Journal of Advanced Research and Reports*, vol. 19, no. 3, pp. 179-200, 2025. [CrossRef] [Google Scholar] [Publisher Link]

[2] Jin Qu et al., "Rising Damp in Heritage Sites under Urban Expansion: A Comprehensive Case Study of the Jinsha Earthen Site," *Building and Environment*, vol. 265, 2024. [CrossRef] [Google Scholar] [Publisher Link]

[3] Eladio Alexander Huamanyauri Cuellar, and Joel Kevin Portilla Serna "*Proposal for an Architectural Concrete Enhanced with Beetroot Fibers to Improve Resistance to Salts in Buildings Located in the Marine Environment Zone of Metropolitan Lima*," Thesis, Peruvian University of Applied Sciences, 2022. [Google Scholar] [Publisher Link]

[4] Peru: Yearbook of Environmental Statistics 2023, National Institute of Statistics and Informatics, pp. 1-581, 2023. [Online]. Available: https://cdn.www.gob.pe/uploads/document/file/5588186/4963255-peru-anuario-de-estadisticas-ambientales-2023%282%29.pdf?v=1706036917

[5] Domenico Giaccone, Ulderico Santamaria, and Marco Corradi, "An Experimental Study on the Effect of Water on Historic Brickwork Masonry," *Heritage*, vol. 3, no.1, pp. 29-46, 2020. [CrossRef] [Google Scholar] [Publisher Link]

[6] Nicholas Fobbe et al., "Drying of Gypsum Plaster Prisms: Prevention of Visible Sodium Sulfate Efflorescence through Calcium Formate Addition," *Materials and Structures/Materiaux et Constructions*, vol. 56, pp. 1-16, 2023. [CrossRef] [Google Scholar] [Publisher Link]

[7] Kristin Balksten, and Paulien Strandberg-de Bruijn, "Understanding Deterioration due to Salt and Ice Crystallization in Scandinavian Massive Brick Masonry," *Heritage*, vol. 4, no. 1, pp. 349-370, 2021. [CrossRef] [Google Scholar] [Publisher Link]

[8] A. Del Puente, Old Houses Collapse Due to Dampness, Panamericana, 2025. [Online]. Available: https://panamericana.pe/eldominical/locales/416307-viviendas-antiguas-colapsan-humedad-20-familias-salir-afectadas

[9] J. Zapata, "Dampness in Your Home? A Senamhi Expert Explains How to Combat it in Winter, Peru21, 2025. [Online]. Available: https://peru21.pe/lima/humedad-en-casa-experto-del-senamhi-te-explica-como-combatirla-en-el-invierno/

[10] National University of Engineering Faculty of Civil Engineering Peruvian Japanese Center for Seismic Research and Disaster Mitigation Budget Program, Cismid – Uni. [Online]. Available: https://www.cismid.uni.edu.pe/cismid-2/

[11] Peru: Characteristics of Private Dwellings and Households - Access to Basic Services. INEI, 2025. [Online]. Available: https://m.inei.gob.pe/prensa/noticias/en-el-pais-existen-mas-de-diez-millones-de-viviendas-particulares-censadas-10893/

[12] Economic Report on Construction, No. 9 - July 2016, Institute of Construction and Development (ICD), Lima, Peru, Peruvian Chamber of Construction (CAPECO), 2016. [Online]. Available: https://iec.capeco.org/descargas/IEC09_0716.pdf

[13] Dana Garlet Arauco-Quispialaya et al., "Automatic Temperature Control System for the Firing of Bricks in the Company "Ladrillera el Toro S.A.C,"" *2023 3rd International Conference on Computer, Control and Robotics (ICCCR)*, Shanghai, China, pp. 303-308, 2023. [CrossRef] [Google Scholar] [Publisher Link]

[14] Roy Moises Ticsihua Taipe, "*Pressed Bricks Made from a Combination of Hardened Cement and Clay from the Quarries of the San Agustín-Huancayo-Junín District*," Thesis, Continental University, Huancayo, Peru, pp. 1-104, 2025. [Google Scholar] [Publisher Link]

[15] Celestino Palomino Pozo, and Fabian Melchor Portocarrero Romero, "*For the Production and Marketing of Vibrated Concrete Blocks Aimed at the Population of Lower Resources Socioeconomic Level "C": San Juan de Lurigancho District*," Thesis, Peruvian University of Applied Sciences, Lima, Peru, 2017. [Google Scholar] [Publisher Link]

[16] Itzel Lopez-Carreon et al., "Moisture Ingress in Building Envelope Materials: (II) Transport Mechanisms and Practical Mitigation Approaches," *Buildings*, vol. 15, no. 5, pp. 1-26, 2025. [CrossRef] [Google Scholar] [Publisher Link]

[17] Qiuling Xiong et al., "Review on the Application Research of Covers with Capillary Barrier Effects," *Journal of Research in Science and Engineering*, vol. 7, no. 1, pp. 125-139, 2025. [CrossRef] [Google Scholar] [Publisher Link]

[18] Elisa Franzoni, "State-of-the-Art on Methods for Reducing Rising Damp in Masonry," *Journal of Cultural Heritage*, vol. 31, pp. S3-S9, 2018. [CrossRef] [Google Scholar] [Publisher Link]

[19] Julie Desarnaud et al., "Effectiveness of Electromagnetic and Electro-Osmosis Methods for the Treatment of Rising Damp," *1st International Conference on Moisture in Buildings*, UCL London, 2021. [CrossRef] [Google Scholar] [Publisher Link]

[20] Jacopo Melada et al., "Does Electro-Osmosis Work in Moisture Damage Prevention? Applicability of Infrared-Based Methods to Verify Water Distribution Under Electric Fields," *Journal of Cultural Heritage*, vol. 31, pp. S38-S45, 2018. [CrossRef] [Google Scholar] [Publisher Link]

[21] Aliihsan Koca, Mehmet Nurettin Uğural, and Ergün Yaman, "Rising Damp Treatment in Historical Buildings by Electro-Osmosis: A Case Study," *Buildings*, vol. 14, no. 5, pp. 1-22, 2024. [CrossRef] [Google Scholar] [Publisher Link]

[22] Alice Roza, "A Case Study of Electro-Osmosis for Rising Damp Treatment in Historical Buildings," *Journal of Civil and Environmental Engineering*, vol. 14, no. 3, pp. 1-2, 2024. [Publisher Link]

[23] Naser Eslami et al., "Experimental Study of Electroosmosis and (Cl-) Diffusion in Fired-Clay Bricks," *Construction and Building Materials*, vol. 447, pp. 1-10, 2024. [CrossRef] [Google Scholar] [Publisher Link]

[24] Pablo Daniel Benítez Mongelós, and Fabiana Belen Silvero, Viability of Electro Osmosis for the Moisture Treatment in Stone Walls, Proceedings of the XII International Conference on Structural Repair and Rehabilitation (CINPAR 2016), Porto, Portugal, 2016. [Online]. Available: https://www.researchgate.net/publication/309349559_Viability_of_Electro_Osmosis_for_the_moisture_treatment_in_stone_walls

[25] Folke Björk et al., "Electroosmosis - A Method Applied for Handling of Moisture in Foundations," *E3S Web of Conferences*, vol. 172, pp. 1-5, 2020. [CrossRef] [Google Scholar] [Publisher Link]

[26] Jianming Ling et al., "Performance Comparison of Different Electrode Materials for Electro-Osmosis Treatment on Subgrade Soil," *Construction and Building Materials*, vol. 271, 2021. [CrossRef] [Google Scholar] [Publisher Link]

[27] Silvio Huayanay Lliuyacc, Hector Elmer Quispe Ruiz, "*Evaluation of Concrete Permeability Using Different Types of Cement for Single-Family Homes in Punta Hermosa*," Bachelor's Thesis, Peruvian University of Applied Sciences, 2025. [Google Scholar] [Publisher Link]

[28] R. Castro Mendoza, "*Disaster Risk Assessment for Natural and Anthropogenic Hazards in the Urban Area of the Punta Hermosa District*," Thesis, National University of San Marcos, 2014. [Google Scholar]

[29] Hugo Fernando Peixoto Macas, and Sergio Jhonatan Aparco Ccancce, "*Areas Affected in the Malanche Ravine, Due to the Activation of the Seco River in Punta Hermosa, using a Hydrodynamic Model*," U.G. Thesis, Peruvian University of Applied Sciences, 2024. [Google Scholar] [Publisher Link]

[30] Anna Kaczmarek, and Maria Wesołowska, "Factors Affecting Humidity Conditions of a Face Wall Layer of a Heated Building," *Procedia Engineering*, vol. 193, pp. 205-210, 2017. [CrossRef] [Google Scholar] [Publisher Link]

[31] Jinpeng Feng et al., "A Novel Humidity Self-Regulating Interior Wall Coating Composite based on Red Mud Derived from Alumina Production," *Construction and Building Materials*, vol. 349, 2022. [CrossRef] [Google Scholar] [Publisher Link]

[32] Nicola Tarque, and Daniel Quiun, "Experimental Tests of Strengthened Small Masonry Walls Made of Horizontally-Hollow Bricks ('Pandereta') in Seismic Zones," *Conference Contribution, 14th Canadian Masonry Symposium, Montréal*, Canada, 2021. [Publisher Link]

[33] Roberth Jackson Atencia Ariza, and James Andres Ramos Herrera, "*Experimental Evaluation of Unconfined Walls of Hollow Brick Laid in a Vaulted Position*," Bachelor's Thesis, Saint Ignatius of Loyola University, 2024. [Google Scholar] [Publisher Link]

[34] Sixto Melanio Alvarado Sullca, "*Mechanical Properties of Masonry Made with Fiberglass-Reinforced Hollow Bricks in Pisco, 2022*," Thesis, National University of Central Peru, 2024. [Google Scholar] [Publisher Link]

[35] Pirámide 12 Concrete Block, Pirámide Bricks, 2023. [Online]. Available: https://www.ladrillospiramide.com/productos/bloqueta-12-piramide/

[36] R. M. Sotelo Carhuachin, "*Structural Behavior of 18-Hole King Kong Brick and Mortar in Confined Masonry Prisms, San Martín de Porres – 2020*," Bachelor's Thesis, Cesar Vallejo University, 2020. [Google Scholar] [Publisher Link]

[37] Marlo Diego Moreno Torres, "*Quality Control of King Kong 18-Hole Brick Types on Their Mechanical, Physical and Chemical Properties, Trujillo 2018*," Bachelor's Thesis, Private University of the North, Trujillo, Perú, 2021. [Google Scholar] [Publisher Link]

[38] Aceros Arequipa, "*Build Safe: Owner's Manual*," Technical Manual, Aceros Arequipa, Lima, Perú, 2020. [Google Scholar]

[39] Bricks for Load-Bearing Walls, Technical Sheet, Aceros Arequipa, Lima, Perú, 2020. [Online]. Available: https://www.acerosarequipa.com/manuales/manual-de-construccion-para-propietarios/los-ladrillos

[40] King Kong 30 Pyramid, Pyramid Bricks, 2024. [Online]. Available: https://www.ladrillospiramide.com/productos/king-kong-30-piramide/

[41] National Building Regulations, Proposal for Standard E.070 Masonry, National Training Service for the Construction Industry (SENCICO), Ministry of Housing, Construction and Sanitation,Republic of Peru, 2019. [Online]. Available: https://www.cip.org.pe/publicaciones/2021/enero/portal/e.070-alba-ileria-sencico.pdf

[42] Saeed M. Al-Tarbi et al., “Development of Eco-Friendly Hollow Concrete Blocks in the Field Using Wasted High-Density Polyethylene, Low-Density Polyethylene, and Crumb Tire Rubber,” *Journal of Materials Research and Technology*, vol. 21, pp. 1915-1932, 2022. [CrossRef] [Google Scholar] [Publisher Link]

[43] Wallison Angelim Medeiros, Guilherme Aris Parsekian, and Armando Lopes Moreno, “Residual Mechanical Properties of Hollow Concrete Blocks with Different Aggregate Types after Exposure to High Temperatures,” *Construction and Building Materials*, vol. 377, 2023. [CrossRef] [Google Scholar] [Publisher Link]

[44] Joseph Dgheim et al., “Enhancements in Hollow Block Technology: Comprehensive Thermal and Mechanical Characterizations,” *Energies*, vol. 17, no. 23, pp. 1-18, 2024. [CrossRef] [Google Scholar] [Publisher Link]

[45] Wall Block 14, Technical Specifications, Pacasmayo, 2021. [Online]. Available: https://construproductos.com/producto/bloque-pared-14-aNqcD

[46] Felice Saviano, Gian Piero Lignola, and Fulvio Parisi, “Experimental Compressive and Shear Behaviour of Clay Brick Masonry with Degraded Joints,” *Construction and Building Materials*, vol. 452, pp. 1-14, 2024. [CrossRef] [Google Scholar] [Publisher Link]

[47] Abed Soleymani, Mohammad Amir Najafgholipour, and Ali Johari, “An Experimental Study on the Mechanical Properties of Solid Clay Brick Masonry with Traditional Mortars,” *Journal of Building Engineering*, vol. 58, 2022. [CrossRef] [Google Scholar] [Publisher Link]

[48] Construex Peru, Ladrillo Macizo King Kong, 2021. [Online]. Available: https://www.construex.com.pe/exhibidores/ladrillera_mvf/producto/ladrillo_macizo_king_kong

[49] Alugunuri Raghu et al., “Enhanced Heat Transfer and Flow Control in Oldroyd-B Hybrid Nanofluids: A Study on Electro-Osmosis Effects and Thermal Characteristics,” *Results in Engineering*, vol. 27, pp. 1-15, 2025. [CrossRef] [Google Scholar] [Publisher Link]

[50] Kangwei Tang et al., “Moisture Migration and Electric Distribution of Unsaturated Clay under Electro-Osmosis with Carbon Fiber Tape As Electrode,” *Engineering Geology*, vol. 294, 2021. [CrossRef] [Google Scholar] [Publisher Link]

[51] Materials Testing Manual, Ministry of Transport and Communications, 2016. [Online]. Available: https://www.slideshare.net/slideshow/manual-ensayo-de-materiales/67429586

[52] Shan Ali Khan et al., “Mathematical and Artificial Neural Network Modeling to Predict the Heat Transfer of Mixed Convective Electroosmotic Nanofluid Flow with Helmholtz-Smoluchowski Velocity and Multiple Slip Effects: An Application of Soft Computing,” *Case Studies in Thermal Engineering*, vol. 61, pp. 1-24, 2024. [CrossRef] [Google Scholar] [Publisher Link]

[53] Aravind Krishnamoorthy et al., “Dielectric Constant of Liquid Water Determined with Neural Network Quantum Molecular Dynamics,” *Physical Review Letters*, vol. 126, no. 21, 2021. [CrossRef] [Google Scholar] [Publisher Link]

[54] Marlene Schmid, and Johann Plank, “Interaction of Individual Meta Clays with Polycarboxylate (PCE) Superplasticizers in Cement Investigated via Dispersion, Zeta Potential and Sorption Measurements,” *Applied Clay Science*, vol. 207, 2021. [CrossRef] [Google Scholar] [Publisher Link]

[55] Cesare Malosso et al., “Viscosity in Water from First-Principles and Deep-Neural-Network Simulations,” *NPJ Computational Materials*, vol. 8, pp. 1-10, 2022. [CrossRef] [Google Scholar] [Publisher Link]

[56] Moisture Meter for Wood, Paper and Walls, Technical sheet, Grupo C&M, 2020. [Online]. Available: https://www.grupocym.pe/cms/_imgs/ficha/FICHA-TECNICA--MEDIDOR-DE-HUMEDAD-PARA-MADERA,-PAPEL-Y-PARED(MATERIAL.pdf

[57] Afv Tools, s.f, Sodimac [Online]. Available: https://www.sodimac.com.pe/sodimac-pe/articulo/128334475/Higrometro-Medidor-de-Humedad-Digital-para-Madera-Concreto-Drywall/128334476

[58] Peruvian Technical Standard, SOILS. Standard Test Method for the Determination of Soluble Salt Content of Soils and Ground Water Technical Corrigendum 1, INACAL/DN, 2025. [Online]. Available: https://servicios.inacal.gob.pe/cidalerta/biblioteca-detalle.aspx?id=39131

[59] Luong Duy Thanh et al., “Drying of Fluid Saturated Porous Materials by Electroosmosis,” *Current Applied Science and Technology*, vol. 21, no. 1, pp. 26-35, 2021. [CrossRef] [Google Scholar] [Publisher Link]

[60] ASTM C67/C67M-21*: Standard Test Methods for Sampling and Testing Brick and Structural Clay Tile*, ASTM International, 2021. [Publisher Link]

[61] Navaratnarajah Sathiparan, and Udayakumar Rumeshkumar, “Effect of Moisture Condition on Mechanical Behavior of Low Strength Brick Masonry,” *Journal of Building Engineering*, vol. 17, pp. 23-31, 2018. [CrossRef] [Google Scholar] [Publisher Link]

[62] *UNE-EN 771-1:2011+A1:2016 SPECIFICATIONS for Masonry Factory Parts. Part 1: Fired Clay Pieces.*, UNE, 2016. [Publisher Link]

[63] José Wilson Guevara Fustamante, “*Levels of Salts and Efflorescence in Masonry Units Produced in Five Quarries in the District of Bambamarca, Chota, 2022*,” Thesis, National Autonomous University of Chota, 2023. [Google Scholar] [Publisher Link]

[64] Occupational Safety and Health Administration, U.S. Department of Labor, 2015. [Online]. Available: https://www.osha.gov/laws-regs/standardinterpretations/2015-09-04-0

[65] Hamed Layssi et al., “Electrical Resistivity of Concrete,” *Concrete International*, pp. 41-46, 2015. [Google Scholar] [Publisher Link]

[66] T. A. Nguyen et al., "Evaluating the Effectiveness of Wenner Mode Configurations for Resistivity-based Moisture Monitoring in Compressed Earth Bricks," *Engineering, Technology and Applied Science Research*, vol. 14, no. 6, pp. 17657-17664, 2024. [CrossRef] [Google Scholar] [Publisher Link]

[67] Xunli Zhang et al., "Electroosmotic Reinforcement Mechanism and Laboratory Tests of Pulsating Direct Current with a High Energy Efficiency Ratio," *Soils and Foundations*, vol. 64, no. 1, pp. 1-9, 2024. [CrossRef] [Google Scholar] [Publisher Link]